NASA/TM–20205000837/Corrected Copy
NESC-RP-17-01215

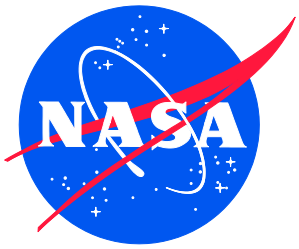

Space Weather Architecture Options to Support Human and Robotic Deep Space Exploration

Joseph I. Minow/NESC and Christopher J. Mertens
Langley Research Center, Hampton, Virginia

Linda Neergaard Parker
Universities Space Research Association, Huntsville, Alabama

John R. Allen
NASA Headquarters, Washington, D. C.

Dan J. Fry and Edward J. Semones
Johnson Space Center, Houston, Texas

Rachel A. Hock
Air Force Research Laboratory, Wright-Patterson Air Force Base, Ohio

Insoo Jun
Jet Propulsion Laboratory, Pasadena, California

Terrence G. Onsager
NOAA Space Weather Prediction Center, Boulder, Colorado

Antti A. Pulkkinen and Chris St. Cyr
Goddard Space Flight Center, Beltsville, Maryland

April 2020

NASA STI Program . . . in Profile

Since its founding, NASA has been dedicated to the advancement of aeronautics and space science. The NASA scientific and technical information (STI) program plays a key part in helping NASA maintain this important role.

The NASA STI program operates under the auspices of the Agency Chief Information Officer. It collects, organizes, provides for archiving, and disseminates NASA's STI. The NASA STI program provides access to the NTRS Registered and its public interface, the NASA Technical Reports Server, thus providing one of the largest collections of aeronautical and space science STI in the world. Results are published in both non-NASA channels and by NASA in the NASA STI Report Series, which includes the following report types:

- TECHNICAL PUBLICATION. Reports of completed research or a major significant phase of research that present the results of NASA Programs and include extensive data or theoretical analysis. Includes compilations of significant scientific and technical data and information deemed to be of continuing reference value. NASA counter-part of peer-reviewed formal professional papers but has less stringent limitations on manuscript length and extent of graphic presentations.

- TECHNICAL MEMORANDUM. Scientific and technical findings that are preliminary or of specialized interest, e.g., quick release reports, working papers, and bibliographies that contain minimal annotation. Does not contain extensive analysis.

- CONTRACTOR REPORT. Scientific and technical findings by NASA-sponsored contractors and grantees.

- CONFERENCE PUBLICATION. Collected papers from scientific and technical conferences, symposia, seminars, or other meetings sponsored or co-sponsored by NASA.

- SPECIAL PUBLICATION. Scientific, technical, or historical information from NASA programs, projects, and missions, often concerned with subjects having substantial public interest.

- TECHNICAL TRANSLATION. English-language translations of foreign scientific and technical material pertinent to NASA's mission.

Specialized services also include organizing and publishing research results, distributing specialized research announcements and feeds, providing information desk and personal search support, and enabling data exchange services.

For more information about the NASA STI program, see the following:

- Access the NASA STI program home page at *http://www.sti.nasa.gov*

- E-mail your question to help@sti.nasa.gov

- Phone the NASA STI Information Desk at 757-864-9658

- Write to:
  NASA STI Information Desk
  Mail Stop 148
  NASA Langley Research Center
  Hampton, VA 23681-2199

NASA/TM–20205000837/Corrected Copy
NESC-RP-17-01215

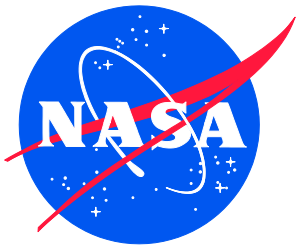

Space Weather Architecture Options to Support Human and Robotic Deep Space Exploration

Joseph I. Minow/NESC and Christopher J. Mertens
Langley Research Center, Hampton, Virginia

Linda Neergaard Parker
Universities Space Research Association, Huntsville, Alabama

John R. Allen
NASA Headquarters, Washington, D. C.

Dan J. Fry and Edward J. Semones
Johnson Space Center, Houston, Texas

Rachel A. Hock
Air Force Research Laboratory, Wright-Patterson Air Force Base, Ohio

Insoo Jun
Jet Propulsion Laboratory, Pasadena, California

Terrence G. Onsager
NOAA Space Weather Prediction Center, Boulder, Colorado

Antti A. Pulkkinen and Chris St. Cyr
Goddard Space Flight Center, Beltsville, Maryland

National Aeronautics and
Space Administration

Langley Research Center
Hampton, Virginia 23681-2199

April 2020

Acknowledgments

The NESC assessment team wishes to thank Dr. Kathryn Whitman and Dr. Shaowen Hu of Johnson Space Center (JSC); Dr. Daniel Heyndericks, United States Air Force (USAF) Research Laboratory (AFRL); and Dr. Piers Jiggens, European Space Agency (ESA) European Space Research and Technology Centre for their support with Task 2. The team would also like to thank peer reviewers Dr. Daniel Dorney, Mr. Steven Rickman, Mr. Jon Holladay, Dr. Robert Hodson, Mr. Steven Gentz, Dr. Morgan Abney, Dr. Leila Mays, and Dr. Ron Turner.

Available from:

NASA STI Program / Mail Stop 148
NASA Langley Research Center
Hampton, VA 23681-2199
Fax: 757-864-6500

NASA Engineering and Safety Center
Technical Assessment Report

Space Weather Architecture Options to Support Human and Robotic Deep Space Exploration

April 1, 2021

Report Approval and Revision History

NOTE: This document was approved at the April 1, 2021, NRB. This document was submitted to the NESC Director on April 5, 2021, for configuration control.

Approved:	*Original Signature on File*	4/6/21
	NESC Director	Date

Version	Description of Revision	Office of Primary Responsibility	Effective Date
1.0	Initial Release	Dr. Joseph I. Minow, NASA Technical Fellow for Space Environments, MSFC	2/13/2020
2.0	Updated Section 11.0, new Finding 15, new Observation 12, revised Recommendation 18	Dr. Joseph I. Minow, NASA Technical Fellow for Space Environments, MSFC	4/1/2021

Table of Contents

List of Figures

List of Tables

Technical Assessment Report

1.0 Notification and Authorization

In his capacity as NASA's Associate Administrator (AA) for the Human Exploration and Operations Directorate (HEOMD), Mr. William H. Gerstenmaier, former AA for HEOMD, requested the NASA Engineering and Science Center (NESC) to conduct an independent technical assessment of space environment monitoring and forecasting architecture options to support human and robotic deep space exploration.

The key stakeholders for this assessment are the HEOMD and Science Mission Directorate (SMD).

2.0 Signature Page

Submitted by:

Team Signature Page on File – 3/26/20

Dr. Joseph I. Minow Date

Significant Contributors:

Dr. Linda Neergaard Parker	Date	Dr. John R. Allen	Date
Dr. Dan J. Fry	Date	Dr. Rachel A. Hock	Date
Dr. Insoo Jun	Date	Dr. Christopher J. Mertens	Date
Dr. Terrence G. Onsager	Date	Dr. Antti A. Pulkkinen	Date
Dr. Edward J. Semones	Date	Dr. Chris St. Cyr	Date

Signatories declare the findings, observations, and NESC recommendations compiled in the report are factually based from data extracted from program/project documents, contractor reports, and open literature, and/or generated from independently conducted tests, analyses, and inspections.

3.0 Team List

Name	Discipline	Organization
Core Team		
Joseph Minow	NESC Lead	NESC/MSFC
Linda Neergaard Parker	Technical Lead	USRA/MSFC
Dan Fry	Space Radiation Analyst	JSC
Chris St. Cyr	Space Environment SME	GSFC
Antti Pulkkinen	Space Environment SME	GSFC
John Allen	Space Radiation SME	HQ/HEOMD
Edward Semones	Space Radiation SME	JSC
Insoo Jun	Space Environment SME	JPL
Chris Mertens	Space Radiation Analyst	LaRC
Terry Onsager	Space Environment SME	NOAA SWPC
Rachel Hock	Space Environment SME	USAF AFRL
Business Management		
Theresa Bardusch	MTSO Program Analyst	LaRC/MTSO
Assessment Support		
Linda Burgess	Planning and Control Analyst	LaRC/AMA
Jenny DeVasher	Technical Editor	LaRC/AS&M
Melissa Strickland	Project Coordinator	LaRC/AMA

3.1 Acknowledgments

The NESC assessment team wishes to thank Dr. Kathryn Whitman and Dr. Shaowen Hu of Johnson Space Center (JSC); Dr. Daniel Heynderickx, United States Air Force (USAF) Research Laboratory (AFRL); and Dr. Piers Jiggens, European Space Agency (ESA) European Space Research and Technology Centre for their support with Task 2. The team would also like to thank peer reviewers Dr. Daniel Dorney, Mr. Steven Rickman, Mr. Jon Holladay, Dr. Robert Hodson, Mr. Steven Gentz, Dr. Morgan Abney, Dr. Leila Mays, and Dr. Ron Turner.

4.0 Executive Summary

Since the final human Moon landing in 1972, all human space exploration has taken place in low-inclination low Earth orbit (LEO), where the Earth's magnetosphere provides relative protection from harmful space radiation. In the near future, as humans return to the Moon, existing scientific and operational ground- and space-based assets should provide sufficient warning of sporadic eruptions from the Sun. But for journeys beyond cislunar space, new monitoring infrastructure and operational procedures will be required to protect astronauts from space radiation hazards. Therefore, infrastructure at cislunar space can serve as a testbed for these future needs.

Understanding solar energetic particle (SEP) event characteristics is critical to the proper design of human and robotic space missions. This report details a study of operational response time for monitoring space weather for crewed flights, specifically targeting lunar and Mars missions. The NESC assessment team evaluated the required minimum latency for data streams and forecasts that will directly affect mission operations using a 41-year database (i.e., European Space Agency (ESA) Solar Energetic Particle Environment Modeling (SEPEM) RSDv2.0) of SEP events. The database contained 192 SEP events that resulted in a dose increase above background levels. Of those, 10% were "multiple events," or events that occurred in quick succession. The analysis provides probabilistic values for time to peak flux and dose rate for the duration of each event. This NESC assessment also evaluated the SEP threshold levels for exploration missions to determine the relevant energy range of required proton measurements.

Accurate modeling and prediction of SEPs is a major challenge, and the performance of available models leaves room for improvement. However, promising paths for predictive SEP modeling have been identified and are actively being explored by the space weather community.

The NESC assessment team performed a detailed review of known space weather models, focusing on the types of models needed (i.e., pre-eruption, post-eruption, and transport) and the input/output requirements for each. The models are listed in Appendix A, with an estimated application readiness level (ARL) for each.

This assessment provides an independent evaluation of NASA needs for a robust and cost-effective space weather situational awareness architecture. Operational time line requirements were developed to ensure general mission planning and situational awareness for lunar and Mars missions. Various architectures were developed for lunar and Mars missions, providing different cost categories in the form of instrument packages of increasing ability (i.e., baseline, enhanced, and comprehensive). Finally, the assessment provides a research and development strategy to bridge the time from successful lunar missions to Mars missions. This strategy uses the International Space Station (ISS) and Gateway platforms.

The NESC assessment team recommends specific instrument packages and charged particle measurement requirements, concept of operations development, a research and development strategy for space weather models and instrumentation, and a strategy to use ISS and Gateway as a proving ground for instrument development required for deep-space missions off the Sun-Earth line. These recommendations include ensuring a 10–30 minute warning time for operations and observations and modeling forecasting capabilities of particles with energies of 10 megaelectron volts (MeV)–1 gigaelectron volt (GeV).

5.0 Assessment Plan

The assessment considered near-real-time monitoring assets, space radiation analysis tools, and forecast methods that could support human-vehicle systems for HEOMD and robotic systems for Science Mission Directorate (SMD) missions beyond LEO in the areas of:

- In-situ radiation and remote solar monitoring hardware planned for deployment on exploration vehicles.
- Existing space environment sensors from NASA, the National Oceanic and Atmospheric Administration (NOAA), the Department of Defense (DoD), and other organizations to the greatest extent possible.
- A minimal set of new hardware only where necessary.

The goal of the assessment was to provide the Agency with options for a robust and cost-effective space weather situational awareness architecture that could effectively reduce space radiation risks for crewed and robotic operations in the inner heliosphere in orbits about Earth, cislunar space, and Mars. Space environment models were reviewed and used as key drivers for instrument selection, but validation and performance metrics for each were not assessed. This was considered beyond the scope of the assessment.

6.0 Problem Description, Proposed Solutions, and Risk Assessment

Human and robotic deep space exploration activities at low-inclination LEO are relatively well protected from the charged particle radiation caused by galactic cosmic rays (GCRs) and eruptive solar events. However, as the Agency moves forward with its journey to Mars goals, many key future human space exploration activities will take place outside the Earth's protective magnetic shielding. Space weather hazards (e.g., energetic charged particle radiation) are some of the key challenges that need to be addressed when humans enter the deep space environment.

As recognized in the report, "NASA's Efforts to Manage Health and Human Performance Risks for Space Exploration" [ref. 1], space radiation remains a key risk for humans and an important consideration for robotic deep space exploration. Limited knowledge about degenerative radiation effects is a key concern. While much remains to be learned, it is clear that reasonable risk mitigation will require advanced situational awareness about space environment conditions that lead to radiation exposure. It is likely that as a part of the risk mitigation, some form of crew radiation storm-shelter procedures will be implemented and executed based on real-time and possibly predictive information about the space environment. For example, the current Orion vehicle has plans for a storm shelter using on-board stowed equipment and materials.

The establishment of robust space weather situational awareness will demand the use of combined observations, models, and analyses. Given the complex nature of the space environment, a variety of approaches will be required for an optimal outcome. Further, while leveraging existing interagency and international space weather capabilities, unique human deep space exploration needs and procedures must be considered. Since no prior work on the topic exists, an assessment of space environment monitoring and forecasting architecture options in support of future human space exploration activities was undertaken.

This assessment will provide guidance to the HEOMD on space weather architectures that can reduce threats from ionizing energetic charged particle radiation for human flight activities. It

will also provide information to Agency programs and projects to help protect crew safety and reduce health risks from space radiation effects. There is an ongoing need within the space environments discipline to develop improved methods for using space environment data to support mission operations. As such, HEOMD missions to the Moon, Mars, and cislunar space will benefit directly from this assessment. SMD missions will also benefit, due to the potential for improved space environment monitoring and modeling capabilities to support mission operations and supplementary observations supporting scientific research activities. It is noted that only the SEP component of the radiation risk is addressed in this document. The GCR component of the radiation risk that is slowly modulated by the solar cycle is addressed at the spacecraft shielding level and not considered here.

The technical activities for this assessment included six tasks. They are summarized below and described in detail in the following sections.

Task 1: Review of Previous Material

Review prior/current work on space weather architectures to understand knowledge gaps in fulfilling the requirements (See Section 7.0). The NESC assessment team reviewed available material and identified recommendations. Specifically, the assessment team considered hardware requirements; habitat designs, including storm shelters for crewed missions; and space weather monitoring assets for future missions, using information from NASA, NOAA, and DoD, such as:

- Availability of space weather monitoring assets for future missions.
- National Space Weather Action Plan and Space Weather Operations, Research, and Mitigation activities.
- Human Systems Integration Requirements Constellation Program (CxP) 70044 and Design Specification for Natural Environments (DSNE) CxP 70023 documents.

Task 2: Assessment of Operational Response Time for Space Weather Monitoring

Develop possible operational response sequences for given sets of observations, models, and tools. This would include assessing the data-stream parameters required for decision-making (See Sections 8.1, 9.0).

Task 3: Review of Relevant Forecasting Tools

Develop a catalogue of physics-based and empirical models and tools for use in conjunction with varied observational architectures (See Section 10).

Task 4: Assessment of SEP Threshold Levels for Exploration Missions

Revisit the >10 MeV SEP constraint [ref. 33] to assess whether it is the appropriate proton-level constraint for Lunar Gateway, Human Landing System, Multi-Purpose Crew Vehicle (MPCV) Program, Mars Habitat, and extravehicular activity (EVA). This includes shielding levels, minimum energy for penetration, and how results modify SEP console operations implemented for the ISS.

Recommend appropriate SEP level and required console staffing needed for Lunar Gateway, Human Landing System, MPCV crew module (CM) model shielding, Mars Habitat, and EVA monitoring, if required (See Section 8.2).

Task 5: Development of Space Weather Architectures

Use the latest human deep space exploration scenarios (e.g., cislunar space, Mars, Moon) together with information about possible storm-shelter options to develop observational architectures of varying levels of complexity in support of operational response to major solar events. Architectures include observation locations and instrument types. The assessment will also consider synergies between science needs and operational monitoring (See Section 11).

- Assess current and future satellite assets for observation gaps (e.g., Solar and Heliospheric Observatory (SOHO), NOAA Geostationary Operational Environmental Satellite (GOES) series and Space Weather Forward Observatory).
- Conduct cost/benefit analysis of additional in-situ and remote sensing satellite assets.
- Assess whether existing Sun-Earth assets and real-time radiation monitors are sufficient.

Task 6: Space Weather Architecture Cost Estimates

Develop first-order cost estimates for the space weather architectures developed in Task 5, with an emphasis on the most cost-effective solutions that leverage existing U.S. operational space weather infrastructure. However, cost, feasibility, and operational needs were not addressed in this assessment (See Section 11).

7.0 Background

In the early 1900s, researchers discovered that Earth's atmosphere was being bombarded by radiation. In the 1920s, when instrumented balloon flights showed an increase in radiation with increasing altitude, physicist Robert Millikan coined the term "cosmic rays" to describe the phenomenon. By the 1930s, scientists speculated that these rays originated from supernovae throughout the Milky Way galaxy.

The first report that the Sun could produce and release energetic particles was made by Forbush [ref. 2], using a cosmic ray monitor in suburban Cheltenham, Maryland. He observed three enhancements in ground-based measurements and put forth the idea that the Sun might be the source of the charged particle increases. A decade later, concerted efforts to understand the space environment as part of the International Geophysical Year led to expanded SEP observations from balloons [ref. 3] and spacecraft [ref. 4]. With the new understanding came the realization that human [ref. 5] and robotic explorers [ref. 6] would be susceptible to the effects of radiation.

Together, GCR and SEP form the primary components of naturally occurring space radiation: an isotropic background of GCRs originating from outside the solar system and sporadic SEPs associated with large eruptions from the Sun. A third form of naturally occurring radiation can be found in trapped regions around planets with intrinsic magnetic fields—on Earth, these are called the Van Allen radiation belts after their discoverer, who instrumented NASA's Explorer 1 with a Geiger counter in 1958. Although radiation belts are scientifically interesting because they are modulated by external (i.e., solar wind) and internal (i.e., ionospheric currents) drivers, this study does not address human exposure to them, even though the Power and Propulsion Element segment of Gateway will linger in the radiation belts. A fourth type of radiation of potential concern to NASA is known as secondary, or albedo, radiation. GCRs and SEPs impinging on the atmosphere or surface of a planet or satellite produce secondary radiation, including energetic neutrons, which may contribute significantly to the surface radiation environment to which astronauts and robotic landers might be exposed.

Leaving the protection of the Earth's atmosphere and geomagnetic field, astronauts traveling in deep space are at risk of radiation hazards induced by various high-energy particles ubiquitous in our solar system. While the low flux of GCRs is hard to avoid and may induce stochastic medical effects (e.g., cancers), intense SEP events can cause acute radiation syndrome (ARS) symptoms that could manifest during the missions (i.e., from the first hours to 60 days after exposure). Though analyses indicate that, for crew inside a typical interplanetary spacecraft with an equivalent 10 g/cm^2 aluminum sphere shielding, ARS symptoms would be moderate even in the worst case [ref. 7]. They could compromise the crew's ability to perform required tasks and thus adversely affect mission success [ref. 8]. An example occurred on August 4, 1972, when a SEP event capable of delivering medically significant doses (i.e., >0.1 Gy) occurred between the Apollo 16 and 17 missions. If a spacecraft had encountered such an event in space, or if astronauts had been exposed while on the lunar surface, then analysis indicated the shielding provided by the vehicle walls (3-5 g/cm^2 aluminum equivalent (Al-Eq)) or spacesuits (0.3-0.5 g/cm^2) would have been insufficient to prevent the induction of ARS among the crew [refs. 7, 8].

For more recent missions with longer stays in space, such as on the ISS, where most of the path falls inside the protective magnetosphere, significantly thicker walls (10-15 g/cm^2) are used to ensure crew exposure levels are as low as reasonably achievable (ALARA). Additionally, the NASA Space Radiation Analysis Group (SRAG) maintains a console position in Mission Control for nominal and contingency operations. In the case of an SEP contingency, the console operator would determine the projected exposure from the event and decide whether the crew should take shelter in areas of the ISS that provide greater shielding. If so, SRAG would work with the Flight Control Team to mitigate SEP impact on the crew and minimize the effects on other crew operations.

The ALARA radiation exposure principle, monitored in real time by SRAG, will be used for the MPCV. As future human missions beyond LEO, such as lunar or Mars missions, will be more likely to experience intensive SEPs, it is vital to comprehensively collect knowledge and understanding of space radiation environments and use the best available space weather architectures and predictions to manage and mitigate these risks. The NASA Spaceflight Human-System Standard (NASA-STD-3001) provides requirements for the design, selection, and application of hardware, software, processes, procedures, practices, and methods for human-rated systems. The standard also contains specific information for space weather monitoring.

Not only are human explorers at risk, but the avionics supporting them and the robotic fleet that composes the space-based infrastructure and scientific missions are also vulnerable. Space radiation is a key design parameter for any space mission. Spacecraft must be designed to function (or at least survive) the influence of the expected radiation environment for its design life. Radiation can damage electronics, materials, and sensors/detectors through total ionizing dose (TID), displacement damage dose (DDD), single-event effects (SEE), internal/surface charging, and increasing the radiation-induced noise background. Among these, SEE due to SEP events are particularly important because they can affect spacecraft operation. The DSNE is a key NASA specification that outlines design requirements for human and robotic missions.

7.1 NASA and Early Concerns About Space Radiation

NASA's concern with space radiation as a hazard for exploration stretches back to the earliest days of the Agency. The historian Portree [ref. 9] noted in the late 1950s at Lewis (now Glenn) Research Center: "Explorer 1 and Explorer 3 (launched in March 1958) detected the Van Allen radiation belts surrounding Earth. Their discovery was the first glimpse of an unsuspected reef, rock, or shoal menacing navigators in the new ocean of space. It raised the profile of ionizing radiation as a possible threat to space travelers."

A NASA Technical Note published in 1961 [ref. 10] was a progress report on the problem of "solar beam events and the radiation hazard in space that results from them." This early concern was sufficiently high that an array of space radiation investigations was planned, including high-altitude balloons, sounding rockets, and spacecraft. The latter included the initiation of the Orbiting Solar Observatory Program and a biological program to "make possible a better assessment of the damage of these beams to organisms." Although Anderson [ref. 11] claimed a "fairly reliable estimate" of sunspot maximum was achievable and SEP events could be predicted, he concluded: "It appears impossible to guarantee non-encounter with solar cosmic rays in space excursions lasting much longer than four days. For longer durations, radiation shielding now appears to be the only feasible approach to safety at times of high sunspot number."

During the next few years, conferences on space radiation were held and researchers attempted to understand how and when solar eruptions produced SEPs. Early empirical forecasting techniques for "proton flares" began to appear.

Following the Apollo lunar landings, English et al. [ref. 12] documented the spaceflight rules in effect for crewed missions to the Moon (Figure 7.1-1). They noted that no major SEPs had occurred during an Apollo mission. The warning time for such an event, based on solar flare observations, was less than one hour up to several hours. But because only 20% of the large flares resulted in SEP events, Apollo Program ground operations planned to continue nominal operational procedures until radiation sensors onboard the Apollo CM confirmed that an event was under way. The flight rules, shown in Figure 7.1-1, were to "continue mission" unless an event occurred during pre-launch or while on the lunar surface. To determine individual radiation exposure, each crewmember wore a personal radiation dosimeter with readout, as well as three passive dosimeters.

Condition	Mission phase	Rule	Comments
Major solar flare has been predicted.	All	Continue mission.	
Major solar flare has occurred.			
Unconfirmed particle event has occurred.	All	Continue mission.	Report: particles have not been confirmed. No mission impact is indicated.
Confirmed particle event and SPAN or real-time analyses indicate the MOD will be exceeded during the mission.	Prelaunch	Hold until data analysis indicates that the MOD will not be exceeded.	
	Earth parking	Continue mission. If data analysis indicates that the MOD will be exceeded by a significant amount before mission completion, translunar injection is no-go.	Translunar injection is no-go only if firm computation before go/no-go indicates more than the MOD.
	All other phases	Continue mission. Consideration will be given to early (or extended) transearth injection and inhibiting crew transfer to the lunar module.	
Confirmed particle event and spacecraft telemetry or personal radiation dosimeter read-out projections indicate the MOD will be exceeded during the mission.	Translunar coast	Continue mission. Consideration should be given to entering in next best preferred target point if the total dose can be reduced significantly without increasing total risk to the crew.	Crew should begin personal dosimeter and radiation survey meter read-outs. A projection of greater than the MOD is not required for crew read-outs.
	Lunar orbit	Continue mission. Consider extending lunar orbit stay time if the total dose to the crew would be reduced significantly by lunar shielding.	Hatch-down attitude may be used to reduce the total dose. If a particle event is confirmed, the crew will transfer from the lunar module to the command and service module.
	Lunar stay	Consider reducing the lunar stay time or extravehicular activities if the total dose to the crew can be reduced significantly without increasing the total risk to the crew.	Comparison of command and service module and lunar surface personal radiation dosimeters is advised.
	All other phases	Continue mission.	

Figure 7.1-1. 1973 Rules for Apollo Missions in Case of a Solar Flare Event
(Note: MOD—mission operational dose)

The 1973 NASA Technical Note also described the Solar Particle Alert Network (SPAN), consisting of three multiple-frequency radio telescopes and seven optical telescopes operated under contract to NASA. These observing assets augmented the worldwide Solar Observing and Forecasting Network, operated by the North American Air Defense Command's Solar Forecast Center in Colorado Springs, Colorado. NOAA's Space Disturbance Forecast Center was also a participant, and produced a twice-daily solar forecast. During missions, the SPAN fed

information via teletype directly to a Space Environment Console at the Mission Control Center, where radiation experts would evaluate the data and combine it with other sources.

Since 1973, human ventures into space have been confined to LEO locations like Skylab, Mir, the Space Shuttle, and ISS. Radiation exposures from GCRs and solar eruptions for platforms in LEO were significantly mitigated by the magnetosphere, and astronaut exposures could be closely monitored during longer stays. Shielded areas were identified for extraordinary SEP events, and the crew could return to Earth in case of extreme events. For the MPCV CM, a specific shelter will be constructed from onboard equipment and materials. LEO platforms benefit from Earth-based observatories to monitor solar activity with minimal communications delays. Research in radiation effects on biological systems and in forecasting solar eruptions continue to advance.

The initiation in January 2004 of President George W. Bush's Vision for Space Exploration (VSE) led to a number of activities concerning space radiation. In April of that year, NASA's Sun-Solar System Connection Division (now Heliophysics) chartered a Radiation Working Group to report on our ability to understand and predict the radiation environment. A National Research Council-chartered workshop in October 2005 addressed ways in which the scientific community could support VSE. This resulted in a report, "Space Radiation Hazards and the Vision for Space Exploration," published in 2006 [ref. 13].

At the request of NASA, the National Council on Radiation Protection produced Report Number 153, Information Needed to Make Radiation Protection Recommendations for Space Missions Beyond Low-Earth Orbit [ref. 14]. This report supported the 2006 National Academy of Sciences study with a mission to "evaluate the radiation shielding requirements for lunar missions and recommend a strategic plan for developing the necessary radiation mitigation capabilities to enable the planned lunar architecture." Additionally, researchers were urged to look to the future: "In developing this strategy for lunar missions, the committee will also consider the likely radiation mitigation needs of future Mars missions and give higher priority to research and development alternatives that will enhance NASA's ability to eventually meet those future needs." The committee report, published in 2008, summarized the radiation risks of spaceflight and recommended ways to address them [ref. 15]. From the report:

> *"Accurate and timely information about this environment is required in order to plan, design, and execute human exploration missions. This information consists of estimates or measurements of the time of occurrence, temporal evolution, and spatial distribution of the radiation, as well as the type, maximum intensity, and energy spectrum of the constituent particles. Unfortunately, the prediction and forecasting of solar activity and space weather are severely hampered by incomplete understanding of how the Sun affects interplanetary space and the local environments of Earth, the Moon, and Mars. Scientific progress in this field, leading to accurate long-term and short-term predictions of the space radiation environment, will contribute to the role that solar and space physics scientists can play in human exploration missions."*

8.0 Space Environment Analysis

8.1 Operational Response Time Assessment for Space Weather Monitoring

A reliable estimate of the energetic charged particle environment is critical for mission success. Important and partly coupled characteristics of an SEP event are fluence, peak flux, energy spectrum, time to reach peak flux, time to reach peak dose, and properties of the cumulative dose profile after an event starts, where fluence, flux, and dose are defined in Section 17. Understanding these characteristics is critical to the proper design of human and robotic space missions.

Because of the unpredictable and sporadic nature of SEP events, statistical models are often used to represent the parameters described above. In a study by Jun et al. [ref. 16], the statistics of event fluences, durations, and time intervals between events were investigated using the then-available historical SEP data set obtained from the instruments onboard the IMP-8 spacecraft. Since then, a more comprehensive SEP data set, based on IMP-8 and GOES and identified as Reference Data Set Version 2.0 (RDSv2.0), has become available. It covers 41 years of SEP events, from 1974 to 2015, under a framework of the ESA SEPEM project [ref. 20].

The energy range covered by the data set is 5–289 MeV, and the specific energy channels are listed in Table 8.1-1.

Table 8.1-1. Specific Energy Channels

Note: Energy Range in MeV

Channel	Energy Range
1	5.00–7.23
2	7.23–10.46
3	10.46–15.12
4	15.12–21.87
5	21.87–31.62
6	31.62–45.73
7	45.73–66.13
8	66.13–95.64
9	95.64–138.3
10	138.3–200.0
11	200.0-289.2

The objectives of this statistical study of SEP events were twofold: First, the statistics of peak fluxes, event fluences, durations, and time intervals were revisited using RDSv2.0, following an approach proposed by Jiggens et al [ref. 17]. Second, the statistical analyses of extravehicular proton fluxes and timing parameters for intravehicular doses were performed using the RDSv2.0 data set. The results addressed the statistical properties of key timing parameters for space radiation environment concerning SEP, which was used to guide space weather architectures developed in this document.

8.1.1 Background Subtraction

For this analysis, the SEP events used were identified as a time period with significant increases of energetic proton fluxes above instrumental and environmental background. When an SEP onset occurs, only the particles that cause an increase above background are attributed to the

event. Therefore, to calculate SEP peak flux and fluence, the background particle flux must be removed. For these reasons, it was important to quantify the typical background levels within the RSDv2.0 data set so they could be removed. Due to solar modulation and the inclusion of different instruments in this 41-year data set, the background levels changed with time. It was important to develop a method that determines an accurate background flux at the time the SEP event occurred. The background for one SEP event may not be the same as the background for another event.

These varying background levels for the RSDv2.0 data set were found via the following steps, using the SRAG-developed background-subtraction method:

1. Select only fluxes that are considered "background" by applying a static threshold.
2. Set individual thresholds for each energy channel to remove fluxes that are too high to be background since they were increases due to SEPs. The goal with this step was to generate a set of fluxes that were roughly attributed to the background environment. Figure 8.1-1 shows the application of a static threshold for energy channel 5. The flux in red is attributed to SEPs and was excluded from the background data set. The flux in black was included in this first estimate of the background.

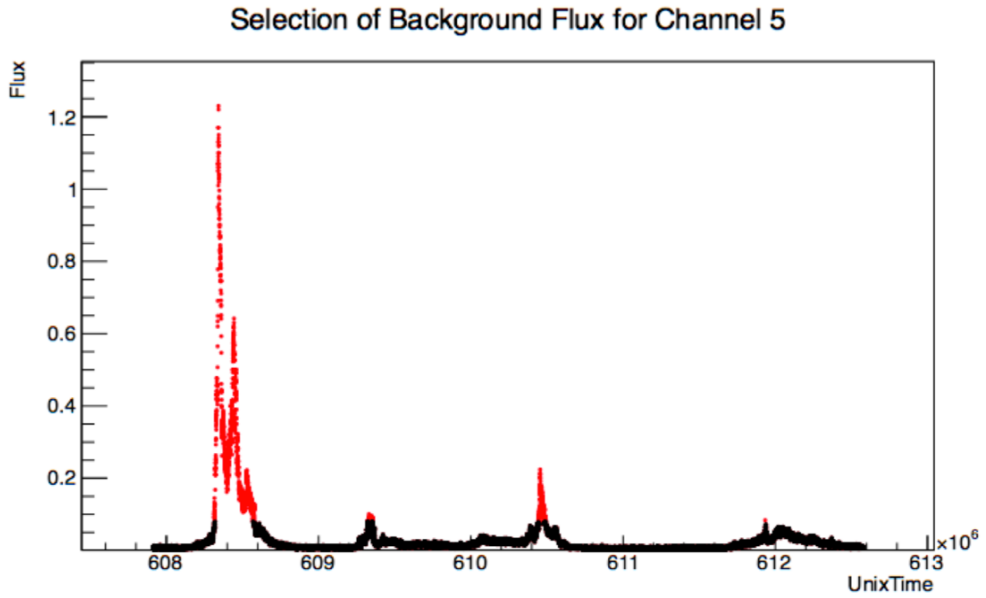

Figure 8.1-1. Application of Static Threshold for Energy Channel 5: 21.87–31.62 MeV

3. Create a distribution of background fluxes for time periods of 3 Bartels rotations (BR) and each channel individually, where BR refers to solar rotation.

By splitting the data into groups of 3 BR (i.e., 81 days), variation of the background with time can be observed. A period of 3 BR contains sufficient data to produce a statistically significant distribution for each energy channel. Figure 8.1-2 shows a distribution for channel 6. A clear peak and a tail extend toward the higher values due to SEP flux present in this initial differentiation between SEP flux and background.

4. Calculate the mean (μ) and standard deviation (σ) of each distribution.

The distributions, such as the one in Figure 8.1-2, were then used to calculate a μ and σ. The μ was interpreted as the average background flux. The σ was interpreted as a measure of fluctuations expected in the background.

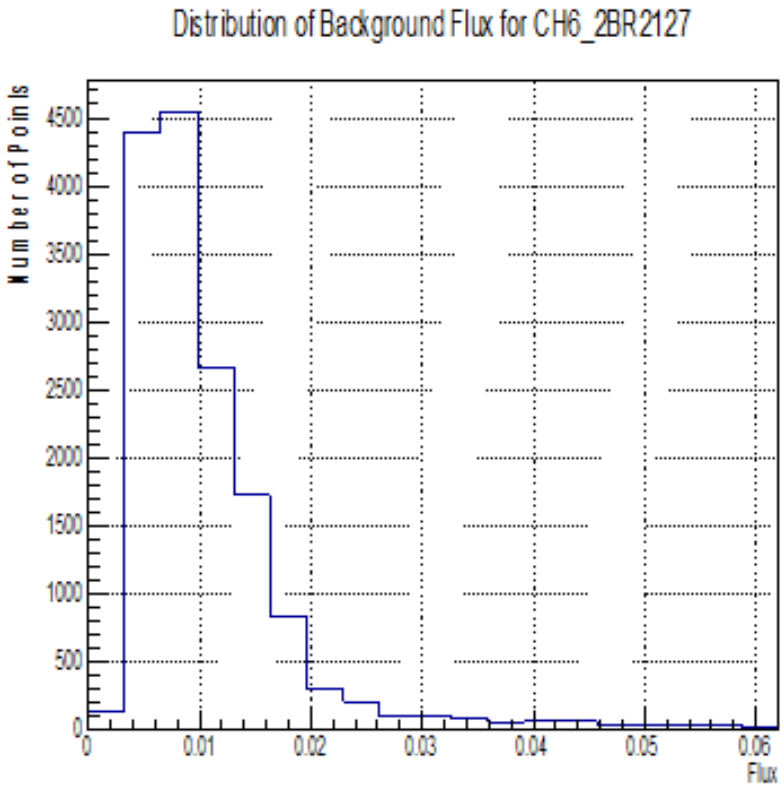

Figure 8.1-2. Distribution for Channel 6: 31.62–45.73 MeV

5. Using the background in step 3 as a changing threshold, iterate steps 1-3. Calculate background for each day using the previous 27 days.

Through an iterative process, the background selection in step 1 was revised by applying a new threshold of $\mu + 3\sigma$ to exclude SEP flux and include background flux. For every day in the RSDv2.0 data set, the previous 27 days of background fluxes were put into a distribution and the average background flux μ and expected background fluctuations σ were calculated. This provided a daily background level and σ for the RSDv2.0 data set, shown in Figure 8.1-3.

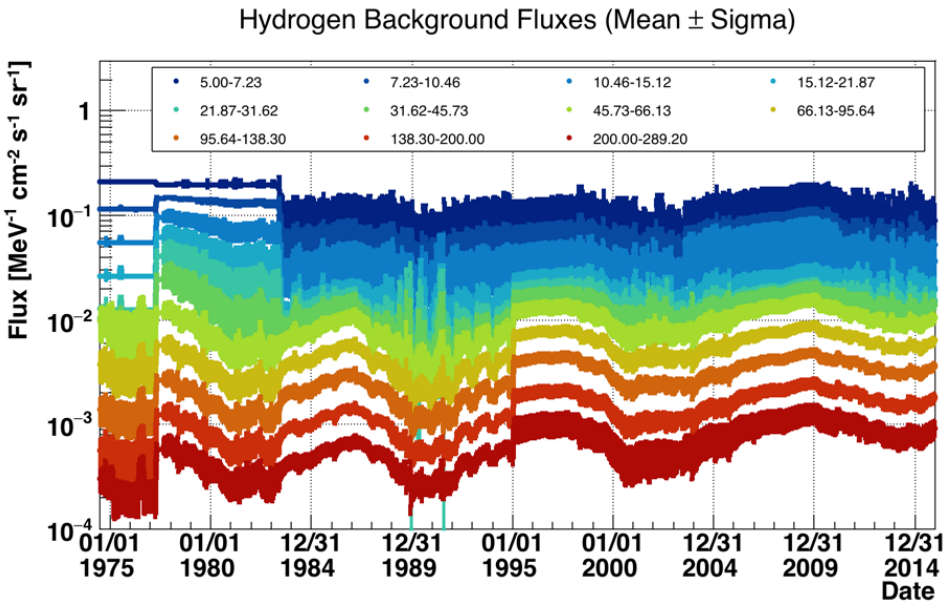

Figure 8.1-3. Daily Background Level and Standard Deviation for RSDv2.0 Data Set

6. Perform a background subtraction to create a clean data set with only SEP flux remaining.

Assume that all fluxes less than $\mu + 3\sigma$ were background, and remove them by setting to 0. Assume that all fluxes above $\mu + 3\sigma$ were the result of SEP events. Subtract the μ to get SEP flux. In Figure 8.1-4, the left image shows the original RSDv2.0 fluxes. The image on the right shows the SEP-only fluxes after the background has been removed. This "clean" data set with the background removed is used to perform the statistical study.

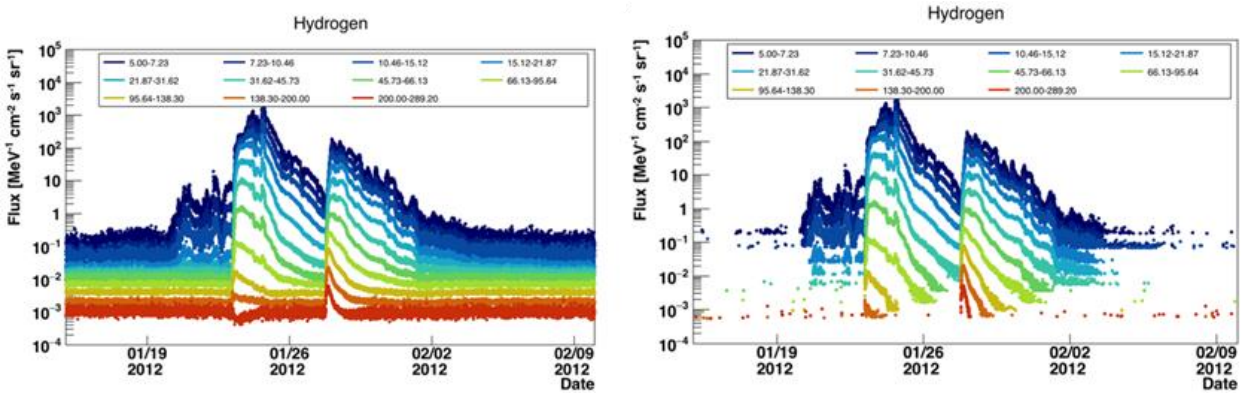

Figure 8.1-4. RSDv2.0 Fluxes

Automated Method to Identify SEP Events in Flux

To calculate SEP start and stop time, it was necessary to generate a set of criteria that would exclude random fluctuations above background (i.e., individual or small clusters of data points that were not real increases due to an SEP).

The criteria selected to identify the start and stop of an SEP event in this background-subtracted data set were as follows:

START in specified channel—each channel treated independently:

- Require flux above background (i.e., non-zero) in specified channel.

- Require any two other channels to detect an increase (i.e., three channels total).
- Require a consecutive increase in three channels for 4 hours.
- Allow a 50-minute gap between the end of one event and the onset of the next to ensure separation of events.
- If all requirements are met, then the SEP event start time was recorded as the first point where conditions are satisfied.

After SEP event starts, allow a gap (i.e., dwell time) of up to 3 hours SEP.

END in specified channel:

- If specified channel and two other channels record no increase in flux during the allowed gap, then the SEP event ends at the last point where all requirements were met.

In Figure 8.1-5, solid lines indicate identified SEP event start times and dashed lines indicate SEP event stop times. Each channel is treated independently, and colors correspond to the energy range in MeV. In some cases, lower-energy channels may identify a single SEP event, while higher-energy channels may increase above and below background multiple SEPs in the same time period.

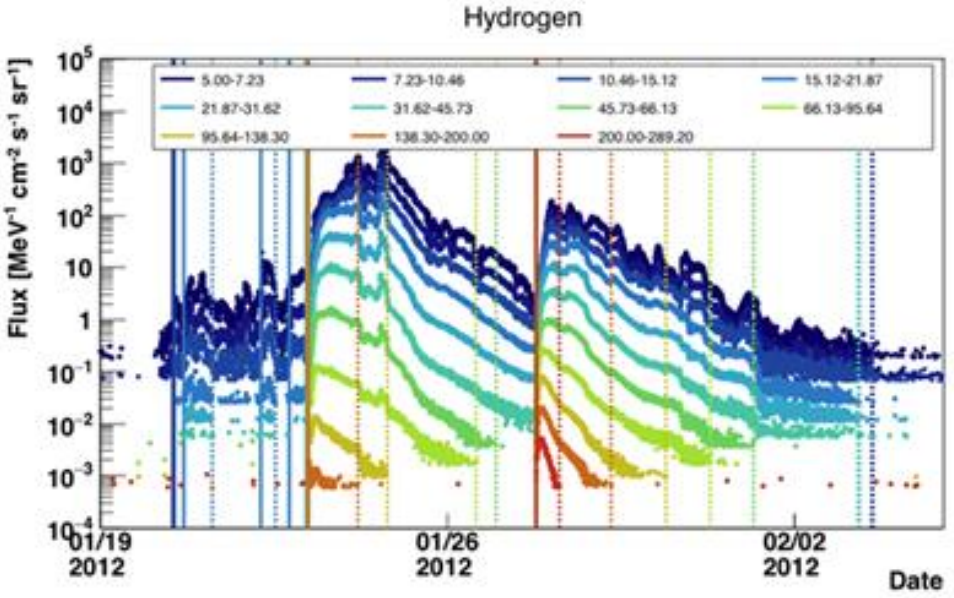

Figure 8.1-5. Proton Fluxes Demonstrating Multiple SEPs in Higher Energies

8.1.2 Identification of Dose-Significant SEP Events

Dose rates were calculated for the original and background-subtracted RSDv2.0 data set by transporting the fluxes through a 10 g/cm^2 aluminum sphere using the HZETRN radiation transport code [ref. 18]. Dose rates were produced for 15-minute periods from 1974 to 2015. While this data set does not include the 1972 SEP, this does not significantly affect the results. The 10 g/cm^2 aluminum sphere approximates the shielding in a typical crewed vehicle. Timing parameters were studied in this way to highlight the energies that contribute most to organ doses. Radiation shielding for EVA suits and lunar surface vehicles with less shielding would require additional analysis.

Transport calculation with the original and background-subtracted fluxes showed that some SEP events did not cause an increase above background inside a typical spacecraft. Only a subset of the SEP events that occurred during the 41-year data set were important for radiation purposes. Figure 8.1-6 shows the dose generated from the original fluxes (blue) and background-subtracted fluxes (red). Note this is the background procedure used by the creators of the SEPEM data sets. Only some of the SEP events would have caused an increase in dose over the background for astronauts inside a vehicle with an equivalent 10 g/cm^2 aluminum sphere shielding.

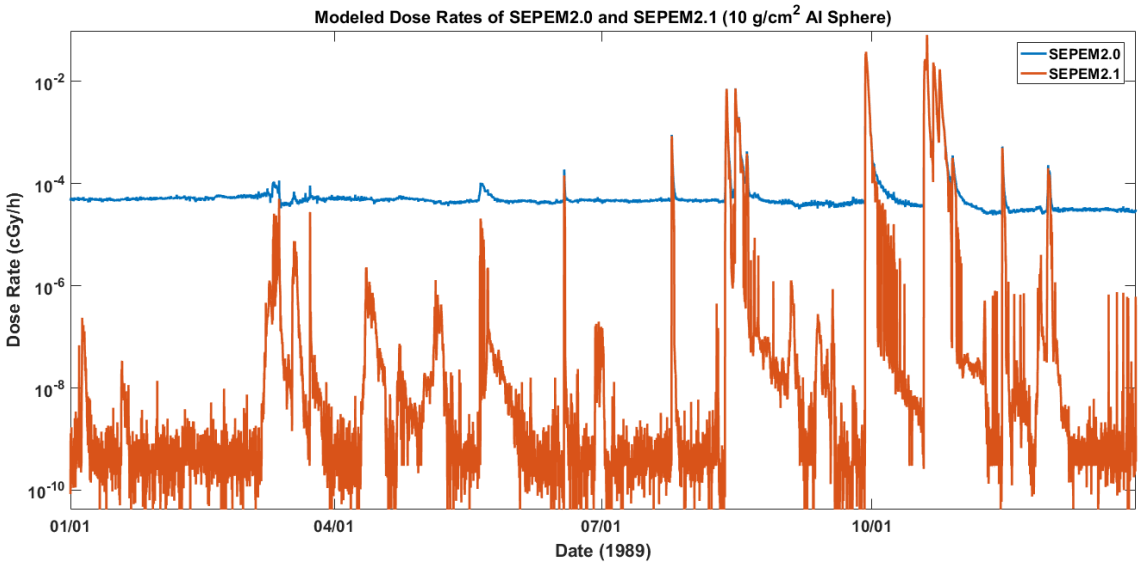

Figure 8.1-6. Radiation Dose Generated from Original Fluxes (blue) and Background-subtracted Fluxes (red)

Comparing the dose rates and the SEP events identified using the background-subtracted fluxes described in the previous section, it was found that the SEP events identified in channel 8 (66.13–95.64 MeV) coincided with the SEP events that showed an increase in dose above background. Figure 8.1-7 shows dose rates for October 1989 with the SEP start and stop times found for channel 8 using the automated identification method. For this reason, the set of SEP events used in this study was taken from the list produced through identification of an increase in flux above background in channel 8.

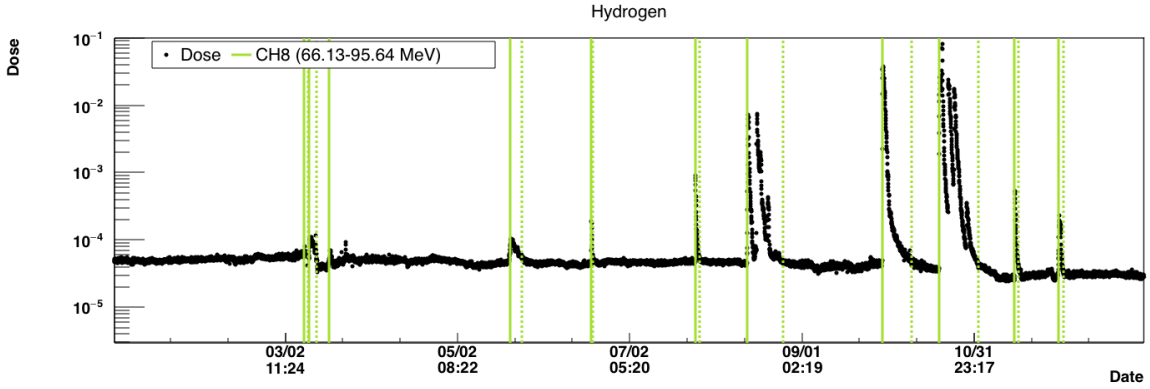

Figure 8.1-7. October 1989 Dose Rates (black) with SEP Start (solid green) and Stop Times (dashed green) for Channel 8

Results

The SEP event list derived from RSDv2.0 channel 8 was used to calculate the following parameters for each radiation-pertinent SEP event:

- Event date
- Onset time
- Event end time
- Duration
- Time between SEP events
- Peak flux for 66.13–95.64 MeV
- Fluence for >66.13 MeV
- Fluence for >95.64 MeV
- Fluence spectrum
- Peak dose rate
- Total dose
- Time to peak flux
- Time to peak dose rate
- Time to 10% dose
- Time to 50% dose
- Time to 90% dose

8.1.3 Ten Largest SEP Events

Results for the 10 largest SEP events were compiled in order of total dose and are shown in Tables 8.1-2 and 8.1-3. Flux and fluence units are [MeV^{-1} cm^{-2} s^{-1} sr^{-1}] and [cm^{-2}], respectively. Dose was calculated for 10 g/cm^2 aluminum sphere. Choice in specific background selection techniques as observed in other data sets results in typical uncertainty of timing of approximately $\pm$30 minutes. The events dated 10/19/89, 1/15/05, 4/15/01, and 8/12/89 consist of multiple SEP events in quick succession.

Table 8.1-2. Ten Largest SEP Events: Flux Summary

SEP Event Date	Onset Time	Duration (Days)	Peak Flux (66.13–95.64 MeV)	Fluence >66.13 MeV	Fluence >95.64 MeV	Time to Peak Flux (66.12–95.64 MeV) (Hr)
10/19/89	13:05:00	13.96	10.9	3.96E+08	1.80E+08	26.3
7/14/00	10:35:00	5.67	10.7	2.79E+08	8.66E+07	5.8
11/8/00	23:40:00	5.93	11.1	2.42E+08	6.30E+07	4
9/29/89	11:50:00	10.45	3.72	1.64E+08	7.38E+07	8
10/28/03	11:20:00	3.93	6.86	2.05E+08	5.66E+07	12.9
11/4/01	16:45:00	5.1	9.83	1.61E+08	3.84E+07	33.6
1/15/05	23:55:00	8.28	10.19	1.14E+08	4.87E+07	103.3
3/7/12	2:00:00	5.58	1.76	8.19E+07	2.62E+07	13.4
4/15/01	14:00:00	5.71	2.47	4.40E+07	2.19E+07	1.7
8/12/89	15:25:00	12.92	1.52	5.40E+07	1.71E+07	13.1

Table 8.1-3. Ten Largest SEP Events: Dose Summary

SEP Event Date	Peak Dose Rate (cGy/Hr)	Total Dose (cGy)	Time to Peak Dose Rate (Hr)	Time to 10% Dose (Hr)	Time to 50% Dose (Hr)	Time to 90% Dose (Hr)
10/19/89	1.15	21.84	26.3	9.8	29.8	134.1
7/14/00	1.19	13.24	2.6	1.8	7.3	23.8
11/8/00	0.956	10.63	4.3	2.5	7.5	16.8
9/29/89	0.58	9.17	8.1	3.6	11.6	28.8
10/28/03	0.48	9.1	13.1	5.1	14.1	42.3
11/4/01	0.672	6.49	33.7	4.9	29.2	36.2
1/15/05	2.04	6.37	103.3	52.3	104.5	113.8
3/7/12	0.187	4.06	13.4	11.2	25.2	47.2
4/15/01	0.512	2.73	1.2	0.9	3.7	65.4
8/12/89	0.104	2.36	85.8	11.8	86.3	119.3

8.1.4 Complete Data Set

Information from all the SEP events was compiled into cumulative distributions and correlation plots and summarized in tables.

8.1.5 Time to Peak Flux and Dose

The cumulative distribution in Figure 8.1-8 shows the time it took for an SEP event to reach 10%, 50%, and 90% dose. These are plotted with the time to reach peak flux and peak dose rate. The plot shows that nearly all events reach 10% dose within tens of hours, and this occurs prior to the SEP peak. However, 90% dose accumulates well after the SEP peak has occurred. The time to peak dose rate and time to peak flux in the 66.13–95.64 MeV channel track well with each other. The time to 50% dose shows a similar curve to the peak flux and peak dose rates.

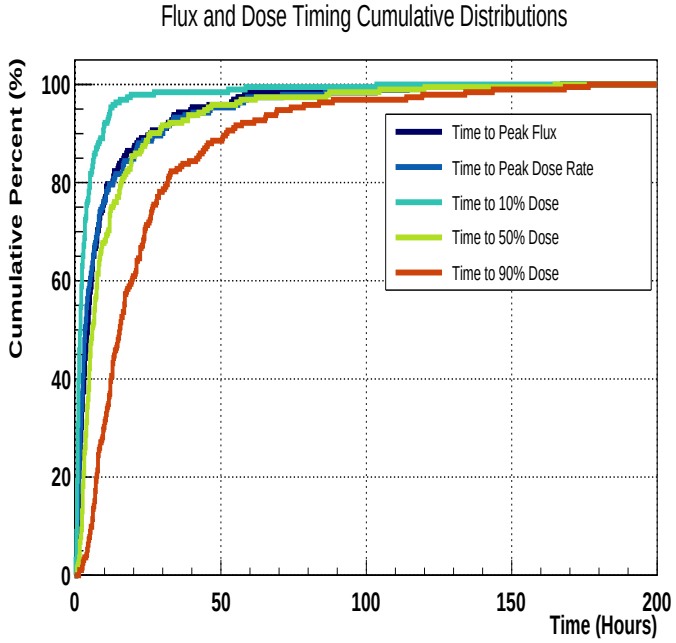

Figure 8.1-8. Flux and Dose Timing Distributions—All Events

Taking a closer look at the accumulated dose and peak flux timing, Figure 8.1-9 shows time to peak flux and time to 30%, 40%, and 50% total dose. For SEP events that reach peak flux in less than about 5 hours, these events reach 30–40% dose around the same time. For events that take longer to reach peak (i.e., after about 20 hours) it can be seen the 50% dose also accumulates around this time. This is an interesting relationship that indicates the 30–50% accumulated total dose occurred at the SEP peak.

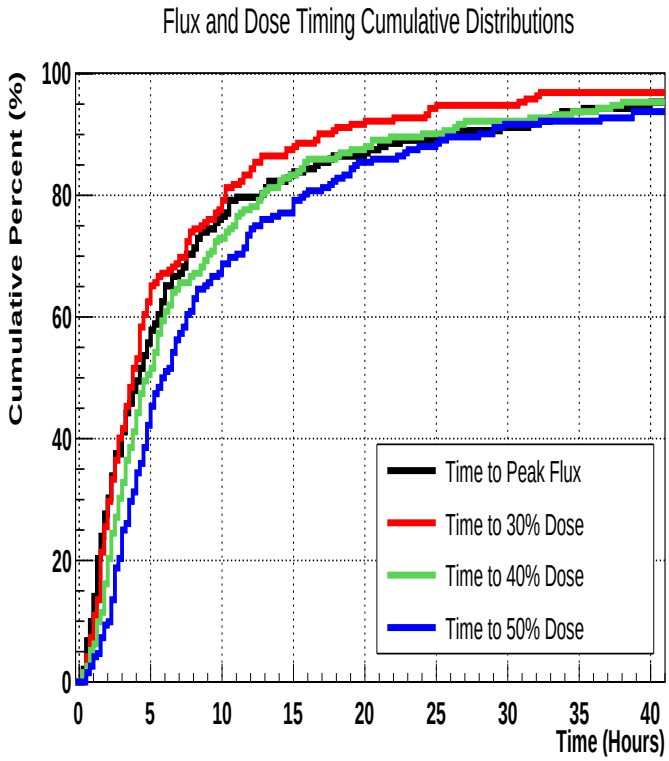

Figure 8.1-9. Flux and Dose Timing Distributions—Quick Rising Events

8.1.6 Cumulative Distribution Analysis for Selected Quantities

Cumulative distributions were used to calculate interesting quantities for the SEP events that contribute to increase in dose behind shielding. Table 8.1-4 shows a selection of operationally critical—with regards to limiting crew exposure—values calculated from the cumulative distributions. The table can be elucidated by looking at the first row: 50% of the SEP events had a duration of 1.625 days or less, 80% of SEP events had a duration of 3.375 days or less, and 90% of SEP events had a duration of 5.625 days or less. Therefore, when an SEP event begins, it is likely to show an increase above background for less than 3 days, and half of the time it will be less than 1.6 days. Looking at the other rows, the table shows that 50% of events reach peak flux within 4.5 hours, peak dose rate within 3.75 hours, and deliver 50% dose within 6 hours.

Table 8.1-4. Cumulative Timing Summary for Operationally Important Quantities

Quantity	10% of SEP Events	Median (50% of SEP Events)	80% of SEP Events	90% of SEP Events
Duration (days)	0.625	1.625	3.375	5.625
Time Interval between SEP Events (days)	2	36	114	196
Time to Peak Flux (hours)	1	4.5	13	26
Time to Peak Dose Rate (hours)	0.75	3.75	13.25	29.75
Time to 10% Dose (hours)	0.25	1.75	5	9.5
Time to 50% Dose (hours)	2	6	16	28.25
Time to 90% Dose (hours)	5.5	15.25	32	52

The data can be interpreted in a different way to understand what happens in the first 10 hours of an SEP event. Table 8.1-5 shows the percentage of SEP events that achieved a certain quantity within 0.5 hour up to 10 hours from the start. For example, within 2 hours, 27.6% of events reached peak flux, 30.3% of events reached peak dose rate, 55.8% of events reached 10% total dose, 9.34% of events reached 50% total dose, and only 1.56% of events reached 90% total dose. However, by 5 hours, 42.2% of SEP events reached 50% dose.

Table 8.1-5. Summary of Event Percentages in First 10 Hours

Hours from Start	Reached Peak Flux	Reached Peak Dose Rate	Reached 10% Total Dose	Reached 50% Total Dose	Reached 90% Total Dose
0.5	2.08%	2.60%	11.50%	0%	0%
1	9.90%	11.50%	32.30%	2.60%	0%
1.5	20.30%	19.80%	46.90%	4.69%	1.04%
2	27.60%	30.70%	55.80%	9.34%	1.56%
5	55.70%	58.30%	79.70%	42.20%	7.29%
10	76.00%	75.50%	92.20%	67.20%	30.70%

8.1.7 Flux-Dose Timing

Figure 8.1-10 shows the time to peak dose rate and time to peak flux plotted for dose-significant SEP events behind shielding. The events (circles) are color-coded according to total dose. The red line indicates a one-to-one timing relationship. The plot shows that larger events tend to reach peak flux and peak dose rate at the same time. The same types of plots may be made for time to peak flux versus different accumulations of total dose. The plots in Figure 8.1-11 show that events reach 10% total dose prior to peak flux, 50% total dose and peak flux in similar amounts of time, and 90% total dose well after the peak has occurred.

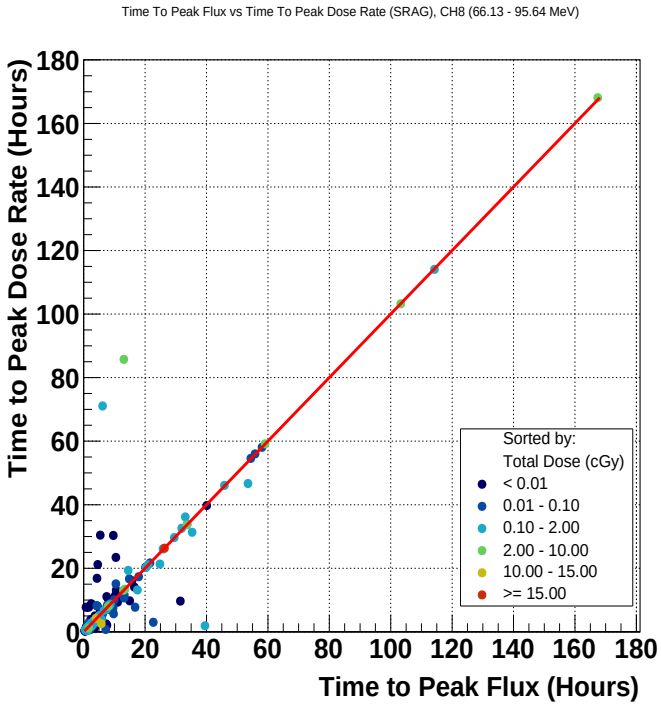

Figure 8.1-10. Peak Dose-Peak Flux Comparison

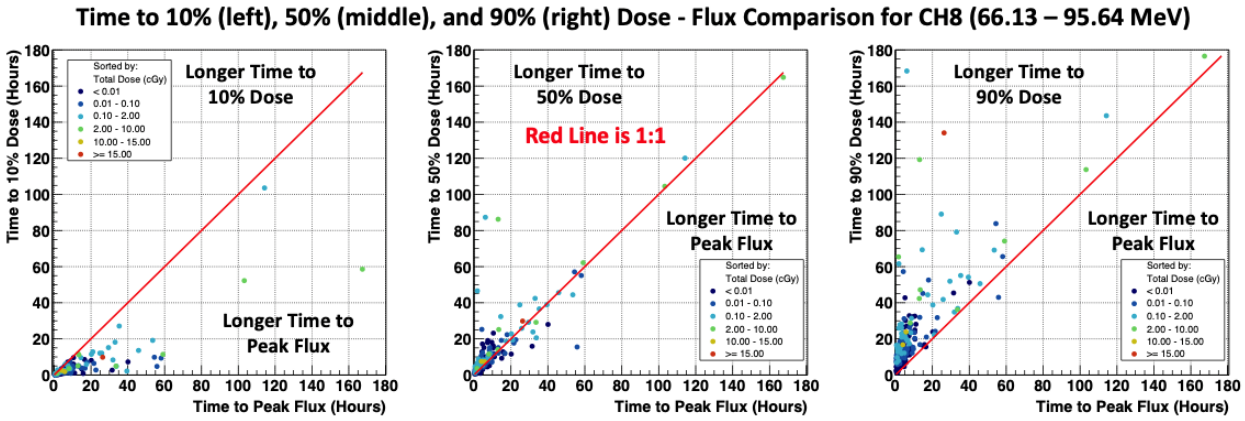

Figure 8.1-11. Percent Dosage-Peak Flux Comparison

8.1.8 Peak Flux and Fluence

A comparison of the peak flux in the 66.12–95.64 MeV channel to the event-integrated fluence in the same channel yields a power-law relationship, shown in the equation:

$$log_{10}(Fluence) = 4.5733 + 1.0623\ log_{10}(Peak\ Flux)$$

8.1.9 Peak Flux and Total Dose

Correlation exists between the peak flux and total dose. As shown in Figure 8.1-12, this study finds the following relationship between peak flux in the 66.12–95.64 MeV channel 8 of the SEPEM data set and total dose inside an aluminum sphere with 10 g/cm^2:

$$log_{10}(Total\ Dose) = 0.1137 + 1.2788\ log_{10}(Peak\ Flux)$$

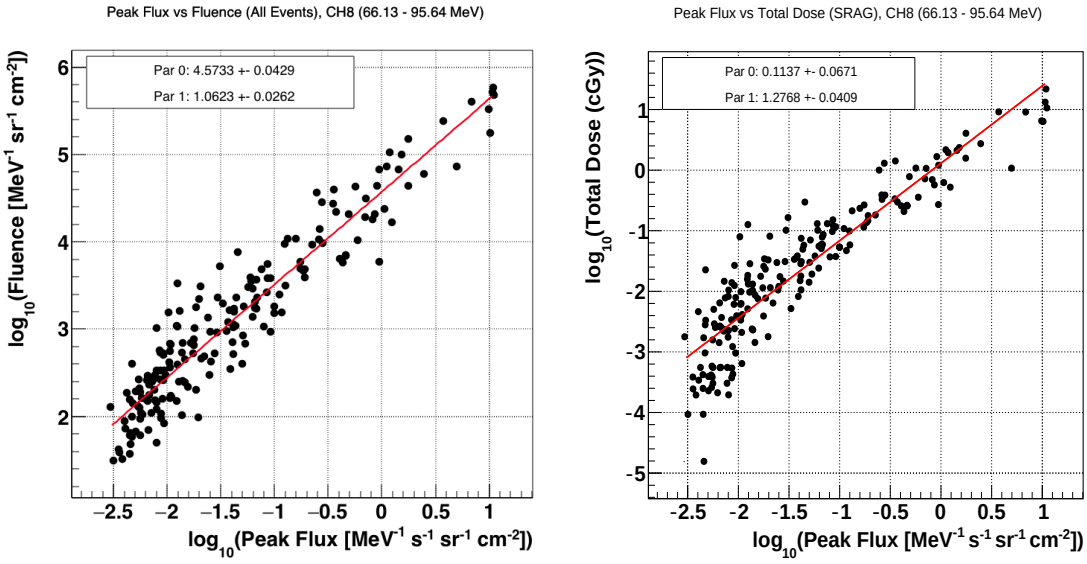

Figure 8.1-12. Correlations Between Peak Flux and Total Dose and Fluence

8.1.10 Discussion

Real-time data streams of space weather parameters are required for space weather situational awareness and decision-making. A timing study was performed to evaluate the required minimum latency for the primary space weather data streams and forecast directly affecting mission operation (e.g., observations of proton flux). Statistical timing quantities related to SEP events were assessed using the European SEPEM RSDv2.0 [ref. 20] data covering 41 years, from 1974 to 2015. This study defined an SEP event as an increase in flux above the environmental and instrumental background. In 41 years, 192 SEP events resulted in an increase in dose above background behind simulated spacecraft shielding (10 g/cm^2 aluminum sphere). Of those, 19 (10%) were multiple SEP events in quick succession, leading to elevated fluxes for up to 13 days. If an SEP event begins, then probabilistic values for duration; time to peak flux and dose rate; and time to 10%, 50%, and 90% dose can be inferred from this study (see Table 8.1.3 of Cumulative Timing Summary for an example). Mitigation actions will be most effective if they occur within the first 2 hours of an SEP event, based on the results in the previous section, which will reduce at least 50% of the SEP dose for a large percentage of events.

The primary mitigation involves an operational response sequence to construct a storm shelter. It is anticipated a shelter can be constructed within 30 minutes, such that proton nowcasting-forecasting should, at a minimum, be available within 2 hours of event onset to ensure maximum potential protection. If the timing and value of the peak flux can be predicted, then it is possible to estimate total dose and can determine whether 10%, 50%, or 90% dose has likely been reached. If an SEP event begins, this study indicates that it will most likely last between 1.5 and 4 days, the peak flux and peak dose rate will likely occur between 4 and 13 hours, 10% dose will likely accrue within 2 and 5 hours, 50% dose will likely accrue within 6 and 16 hours, and 90% dose will likely accrue within 15 and 32 hours.

8.2 Assessment of SEP Threshold Levels for Exploration Missions

Current NASA human spaceflight missions use the NOAA GOES SES platform for monitoring energetic charged particle fluxes. The >10 MeV and >100 MeV integral flux channels play a key role in flight control team actions. Each was continuously monitored for times when the particle flux for these energies crossed the 10 particle flux units (pfu) and 1 pfu levels, respectively. An assessment was performed to determine if the energy range of protons monitored is sufficient for future exploration missions beyond LEO [ref. 19].

Several factors were considered. One, Earth's geomagnetic field provides protection for low-inclination LEO missions by suppressing SEP flux in areas other than high-latitude passes. In free space, this protection will not be available and exploration missions will be affected by the entire duration of a SEP event. Second, the ISS itself provides relatively good protection due to its large shielding mass, which will not necessarily be present for exploration missions beyond LEO. Any assessment must take into account the absence of the geomagnetic field and specific vehicle shielding. Thus, calculations of dose response follow two main avenues:

1. Calculation of instrument point dose equivalent for multiple large SEP events, using ISS and MPCV located at geosynchronous orbit (GEO).
2. Calculation of blood-forming organs (BFO) dose equivalent for multiple large SEP events, using the MPCV located at GEO, including approximate storm shelter mass and body self-shielding.

The assessment used the NOAA GOES satellite due to its location at GEO and its good approximation of free space beyond the protection of the geomagnetic field. Thus, the relatively weak geomagnetic field at GEO does not influence the energetic ions that contribute to human radiation exposure. This allows direct use of GOES proton fluxes. ISS and MPCV were used to give a reference point to ISS in LEO, where there is more than a decade of measurements of instrument point dose inside ISS. It allows for calculations at two extremes in vehicle shielding mass, allowing the assessment of threshold calculation sensitivity to SEP energy. Heavily shielded vehicles will suppress more of the proton flux below 100 MeV in energy than something with lower shielding mass such as MPCV, and a more mass-heavy vehicle will yield more secondary radiation.

8.2.1 Methodology

All calculations were performed as follows: Event-integrated spectra were formed from GOES and Interplanetary Monitoring Platform (IMP) satellite and ground-based neutron data, spanning from 1973 to 2015. All events were pulled from databases developed through other outside efforts and appropriately vetted in the open literature. For example, the SEP measurement data used in the previous section were analyzed and compiled by the ESA's SEPEM effort [ref. 20]. The SEP data used in this section are the spectral parameters derived from the measurement data described by Raukunen et al [ref. 21]. Database details are not discussed in this report. Specifically, spectra in this section were fit to a given analytic expression [ref. 21], and each fit was used to generate input spectra to the HZETRN radiation transport code.

Another important assumption imposed on the analysis of this and the previous section is that the incident SEP particles on the spacecraft are isotropically distributed. It is known that the SEP proton beam for large events is highly collimated along the interplanetary magnetic field line, with a high degree of anisotropy persisting through the peak of the proton flux [refs. 22, 23, 24].

For the MPCV, the BFO dose to a crewmember can be between a factor of 2 to 10 higher or lower than the isotropic assumption, depending on the specific direction of the incident SEP proton beam and the specific crew location [ref. 25]. Efforts are under way to better understand anisotropy effects on human radiation exposure in deep space and to account for spatial anisotropy during SEP events in the real-time assessment of acute radiation risks for the MPCV [ref. 26]. While the magnitude of dose at a particular location within a spacecraft can vary significantly with the degree of anisotropy of the incident SEP proton distribution, the statistical analysis of the threshold quantities presented in this report will not be substantially affected by directional effects.

To assess the contribution to total dose from different energy protons, the fit spectra were modified according to a threshold in proton energy. For example, a dose calculation to determine the contribution from only protons with energy $\geq$100 MeV was performed event-by-event by setting the proton flux at all energy bins <100 MeV to be zero. Calculations were stepped through by changing the energy cutoff for zero flux from 10 MeV to ~1 GeV.

Total dose to the BFOs was calculated from 65 historical SEP events using the MPCV CM design [ref. 26]. The free-space SEP proton spectra of the historical events were parameterized by double power-law fits in kinetic energy to event-accumulated integral fluence measured by the GOES and ground-based neutron monitor data [ref. 21]. This set of events included ground-level enhancements and associated SEPs.

The MPCV has four seated crew locations, and the BFO dose was calculated at each location from a numerical solution of the Boltzmann transport equation using the HZETRN code, which included only forward-propagating neutrons in this application [ref. 26]. The material shielding thicknesses required for performing the transport calculations were determined by ray tracing the MPCV CM computer-aided design (CAD) model. The range of median shielding thicknesses at the four nominal seated crew locations was 32–39 g/cm^2 Al-Eq. The MPCV has provision for the crew to erect a storm shelter within the spacecraft during SEP events. Thus, the range of median thicknesses of the crew locations within the vehicle storm shelter is 36–43 g/cm2 Al-Eq. To calculate BFO dose, the MPCV CAD model of materials and thicknesses were combined in the transport and dosimetric calculations with the tissue and BTO thicknesses of the Male Adult voXel (MAX) and Female Adult voXel (FAX) models of the human body.

The BFO doses presented in Section 8.3.2 are averages of the doses calculated at each crew location for the MAX and FAX models. Moreover, BFO doses are shown for the nominal seated and sheltered crew configurations, providing insight into the shielding effectiveness of the vehicle storm shelter over a broad range of historical SEP events. The BFO doses are reported in units of gray equivalent (Gy-Eq), which is the dosimetric quantity relevant to assessing acute radiation risk (National Council on Radiation Protection, 2000). The Gy-Eq dose is approximated by multiplying the calculated BFO dose (Gy) by the average relative biological effectiveness of protons, which is a factor of 1.5 (Hu et al., 2009).

8.2.2 Results

A single event was used to investigate the effects of different vehicle shielding distributions. Results for the May 2012 event for simulated tissue equivalent proportional counter (TEPC) instrument dose are shown in Figure 8.2-1. Contribution to total dose is shown for three vehicle-shielding configurations (i.e., empty MPCV CM, ISS U.S. Laboratory, and MPCV CM), including the storm shelter and body self-shielding. A relatively steep decline in contribution to

total dose occurs across all shielding distributions as the spectrum cutoff energy increases. The black horizontal line denotes the 10% mark to guide the eye to regions of relatively low dose contribution. Several notable features in the data are:

1. The cutoff energy of the rollover in dose contribution moves to higher proton energies as vehicle shielding increases because increased shielding thickness attenuates the lower energy flux. To quantify the relevant energy regime, the relevant energy range was defined as the cutoff energy corresponding to the 90% and 10% contributions to total dose, or 90/10.
2. An empty MPCV with a single TEPC-like detector showed a 90/10 dose contribution for protons between approximately 30 and 120 MeV.
3. As the vehicle shielding increases (e.g., ISS U.S. Laboratory), the 90/10 proton energy range increased to about 80 to 350 MeV.
4. At the most shielded configuration (orange open circles on the far right), the 90/10 range for this event was roughly 150 to 650 MeV.

MPCV CM and the ISS U.S. Laboratory differ in terms of shielding mass, with the latter having a ray distribution shifted nearly an order of magnitude to higher equivalent aluminum thicknesses over the former. The MPCV CM + storm shelter + body shielding is shifted to the right in Figure 8.2-1, pointing to the importance of including additional shielding from vehicle stowage and the human body to assess the energy range contributing to BFO dose.

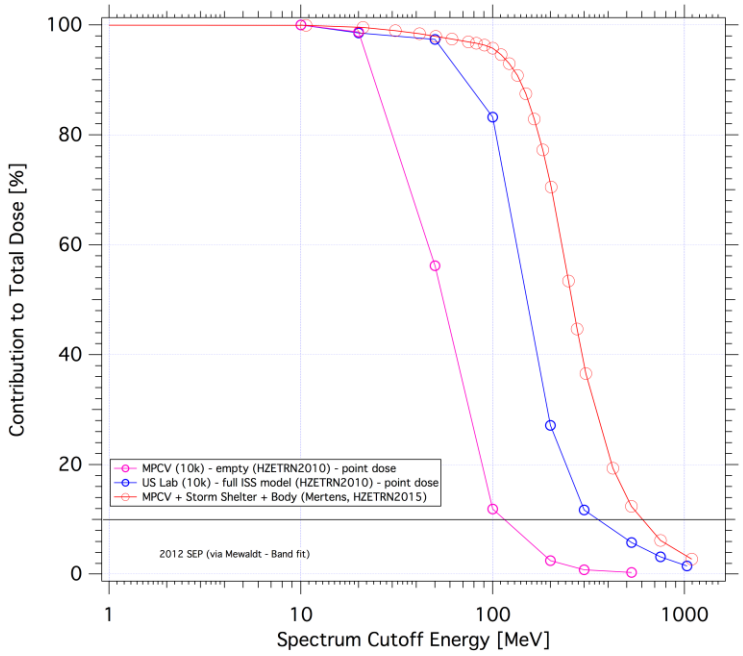

Figure 8.2-1. Proton Energy Contribution to Simulated Instrument Point Dose as a Function of the Minimum Energy of the Free-Space SEP Proton Spectrum Used in the Transport and Dose Calculations

To account for variation over a multitude of SEP events, the same calculation used to produce the results in Figure 8.2-1 was performed for an ensemble of 65 historical SEPs, focusing on MPCV CM as the crew vehicle. Figure 8.2-2 shows the contributions to the total BFO dose from various segments of the free-space proton energy spectrum for the set of historical SEP events. The abscissa points are cutoff energies, defined in this context as the lowest energies of the free-space SEP spectrum, used in the transport and dose calculations. Thus, the ordinate point at each

cutoff energy is the contribution to the total BFO dose arising from the energies of the free-space proton spectrum that are greater than the cutoff energy. For the seated configuration, more than 99% of the total BFO dose comes from proton energies greater than 10 MeV for all historical SEP events. The average and median contributions for proton energies greater than 100 MeV, for example, were ~80% and ~87%, respectively.

The range of contributions to BFO dose from this set of historical SEP events for energies greater than 100 MeV extends from 54% to 95%. Note for comparison that an aluminum slab with a median shielding thickness at the MPCV crew locations would stop all protons with energies less than about 200 MeV. The average and median contributions to BFO dose from proton energies greater than 500 MeV is between 3% and 4%, but the spread in dose contributions was quite large. At the upper end of the dose contributions, nearly 25% of the BFO dose is coming from energies greater than 500 MeV for the spectrally hard February 1956 event.

8.2.3 Summary

The results presented here allow the determination of the most relevant proton energy range future space weather architectures should be capable of measuring. Using the 90/10 metric, Figure 8.2-2 yields an energy range of ~150 to ~650 MeV. This is in good agreement with the results of the average in Figure 8.2-2, shown as a solid red line. However, to incorporate more variance among the ensemble of relatively hard spectra, analyses should include protons with energies up to 1 GeV. A rule of thumb for typical spacecraft shielding is that only protons of energy >30 MeV can penetrate the pressure vessel. Flux increases at these lower energies have for decades served as a signature of adverse space weather conditions, and real-time information on proton flux at energies as low as 10 MeV are valuable for EVA operations.

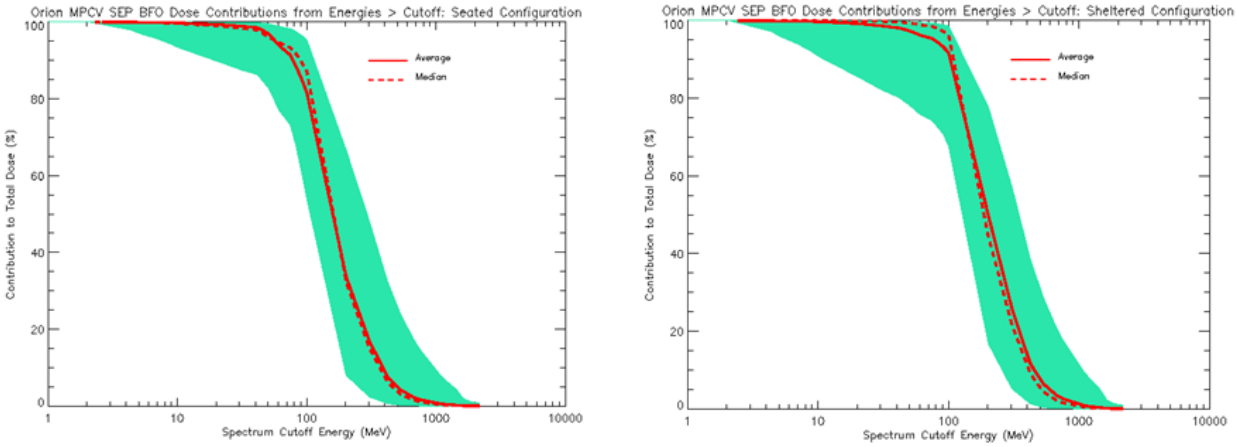

Figure 8.2-2. (Left) Fractional Contribution to Total MPCV BFO Dose as a Function of Free-space SEP Proton Cutoff Energy for (Nominal) Seated Crew Configuration; (Right) Same, but for Sheltered Crew Configuration. Shaded Regions contain Fractional BFO Contributions vs. Cutoff Energies for the Set of 65 Historical SEP Events

The difference between the sheltered and non-sheltered fractional dose contributions in Figure 8.2-2 are small because only 4-5 g/cm^2 (median) of additional shielding (shelter) has been added to the median vehicle shielding of ~ 34 g/cm^2 Al-Eq. This median thickness corresponds to the average range of a 200 MeV proton. The 50% fractional dose contribution for the seated configuration (non-shelter) corresponds to a cutoff energy of about 200 MeV, providing a consistent picture the expectations based on simple proton transport physics. The average range

of a 225-250 MeV proton in aluminum is around ~ 40 g/cm2, which is consistent with the 50% fractional dose contribution for the sheltered configuration with median thickness ~39-40 g/cm2 Al-Eq. In Figure 8.2-1, the 50% fractional dose contribution for the empty MPCV corresponds to a cutoff energy of about 60 MeV. The average range of a 60 MeV proton in aluminum is about 4 g/cm2, consistent with the average depth of an empty spacecraft. In short, the differences between the curves in Figures 8.2-1 and 8.2-2 are consistent with the different shielding thicknesses and consequent effects on the proton transport.

9.0 Operations Timeline

Assessing the concept of operations for the launch, cruise, orbit, and surface phases of lunar exploration produces three components of forecasts and real-time information necessary for the operations team:

1. **General mission planning and situational awareness**, requiring 24-hour all-clear forecasts of >100 MeV protons. All-clear forecasts are defined as the probability of events **not** happening (e.g., of >100 MeV protons **not** exceeding 1 pfu within the forecast window). In addition, 6-hour all-clear forecasts of >100 MeV protons will be useful for launch commitment. For EVAs, 24- and 6-hour all-clear forecasts of >10 MeV protons are needed.
2. **Decision to deploy and enter a storm shelter** or, in the surface phase, to return to lander in the event of solar activity. For this, the probability of an SEP event occurring after an eruption is observed on the Sun is required. If an event is likely, predictions of the SEP event onset time and peak flux are also needed.
3. **Information about the evolution and expected duration of an SEP event**. Once an SEP event begins, forecasting the time profile will provide an estimate of how long the crew will need to shelter.

Nowcasting, or real-time assessment of the energetic particle environment, is the baseline space radiation protection requirement that will be fulfilled by SRAG dosimeters. Each of the three forecasting and information components above requires a different type of forecasting model, driven by a diverse set of observations. General mission planning and situational awareness require all-clear forecasts with 24-hour lead time.

Figure 9.0-1 depicts a hypothetical, but representative time profile for energetic proton flux during an SEP event. The figure indicates the three types of modeling and associated approximate timescales needed to safeguard the crew from SEP-related radiation exposure. The three types of modeling link directly to the three types of information and corresponding actions listed above. The same information is necessary regardless of the mission target, so the discussion pertains equally to lunar and Mars missions.

As Figure 9.0-1 shows, SEP events, model types, and corresponding forecasts can be divided into three broad categories: pre-eruption, post-eruption (e.g., onset and rise to peak flux), and post-eruption time profile (e.g., rise, decay, and end of the event). The latter two can overlap in terms of SEP event time, but the modeling approaches can be quite different.

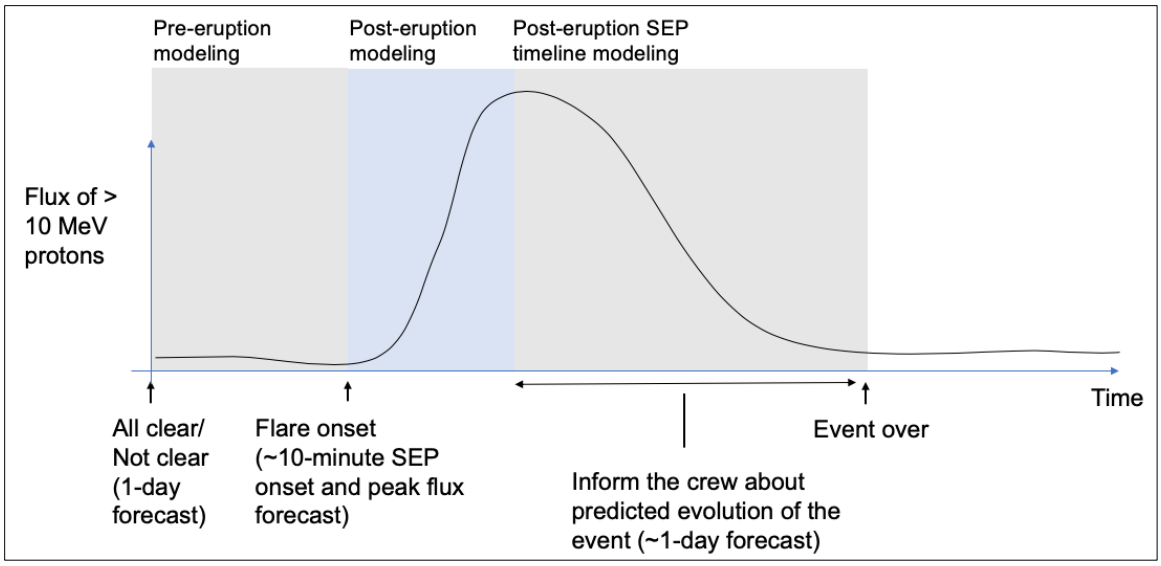

Figure 9.0-1. Illustration of Time Profile for Energetic Proton Flux During SEP Event

As shown in Section 8, the primary concern from the total dose standpoint is events with >100 MeV protons. However, lower-energy events (i.e., >10 MeV protons) can also be a hazard during EVAs. Most of the current SEP prediction models have been tuned for characterizing >10 MeV proton fluxes instead of >100 MeV protons.

In Figure 9.0-1, the first type of modeling along the timeline is the pre-eruption "all-clear." Pre-eruptive modeling and forecasting is used to provide 6- and 24-hour estimates for the likelihood of major solar eruptions that may expose the crew to elevated levels of energetic charged particle radiation. Spacecraft, once launched, or surface EVAs, once initiated, cannot be easily modified if an eruption takes place. Therefore, this type of modeling would be used in EVA planning.

Post-eruption modeling takes place immediately after an eruption has been observed in the solar corona. This type of modeling provides short lead-time predictions of the expected onset of an SEP event near the crew location, and optimally estimates for the expected peak energetic proton flux. "Short lead time" signifies time scales of tens of minutes, which should be considered in the context that it takes sunlight 8 minutes to propagate to 1 astronomical unit (AU). Post-eruption modeling is used to trigger immediate mitigation actions, such as deploying and entering a storm shelter.

The current requirement for deploying a storm shelter is 30 minutes [refs. 7, 34]. The rationale for this requirement follows from the fact that while the rise time and total duration of SEP events has varied for historic events, as discussed in Section 8.1, if assembly time is no more than 30 minutes, the probability of exposure exceeding 250 mGy-Eq to BFO (the current NASA standard) is expected to be low. With the 30-minute requirement, any additional post-eruption predictive information about the pending SEP event will allow early deployment of the shelter and further reduce the crew exposure. This conclusion is supported by the analysis in Section 8.1: For half the events studied in this assessment, 10% of total dose was reached within 1.75 hours into the event. The fastest time to 10% of the dose was 0.9 hour. Consequently, predictive information in 10–30 minute lead-time scales would allow early shelter deployment and minimize crew dose. The usage of predictive information for minimizing crew dose is in alignment with the ALARA principle.

The post-eruption time profile predictions refer to characterization of the temporal evolution of the fluxes once the onset of the SEP event has taken place. This type of predictive modeling will allow informing the crew and mission planning about the expected duration of the event.

10.0 Space Weather Models in Support of Future Human Space Exploration

Numerical models will be an essential component of a space weather architecture. Operational models, together with forecaster expertise, will make possible a comprehensive set of products to reduce space radiation risks. Extensive research and modeling efforts directed at understanding the space environment have produced a broad spectrum of model resources, and now these capabilities must be made operationally available.

While past research has contributed to numerous models for scientific research, few models are used operationally and few have been quantitatively assessed for operational value. Various reasons for this include model development, utilization of test data, and analysis of model output are often implemented with research goals in mind, and it can be unclear how well a model would perform operationally. Model interfaces are often not constructed for generic or real-time use, and therefore cannot easily be used elsewhere or tested against other models. Also, models typically use data selected for specific conditions, often modified to remove gaps or unphysical values. Real-time operations do not allow such preselection of data, but require that a model provide valid output under program-specified conditions. Finally, many available models have been developed internationally and may be difficult to evaluate or obtain for operational use in the U.S.

The model and data resources that exist and are being developed, together with the need for operational space-radiation information, present the imperative to evaluate and efficiently transition a subset of these resources into operational use. Recent activities have highlighted this need and helped focus interagency efforts. In particular, the new National Space Weather Strategy and Action Plan [ref. 27] includes specific actions to enhance space weather models and transition them to operation. These actions will address leveraging existing capabilities and centers, as well as potentially creating a more formal framework.

As discussed in Section 9.0, predictive space environment modeling is needed to support crew radiation protection actions and mission timeline planning. The timeline may include EVAs that are particularly hazardous from the standpoint of exposure to SEP events. Optimally, the modeling would provide pointwise predictive environment characterization at the crew location and more global heliospheric-wide modeling for general situational awareness about conditions associated with energetic charged particle radiation.

This section identifies and reviews models that can support operational SEP mitigation procedures in the context of the Figure 9.0-1 timeline. The key goal is to define observations required for driving the predictive SEP models. The observational requirements are used to define the required instruments and measurement locations (i.e., the core component of space weather architecture). Again, the scope of the assessment included only the SEP hazard. GCR background, responsible for predictable near-constant flux of energetic particles modulated only by the solar cycle, was not considered in this assessment. Given the near-constant background nature of GCRs, the corresponding hazard should be mitigated at the spacecraft shielding design and mission timing level, with respect to solar cycle. GCRs cannot be addressed in the short term

(i.e., hours to days), like acute radiation syndrome mitigation actions (e.g., deployment of temporary storm shelters).

Section 10.1 identifies models capable of providing the required three types of space weather information and indicates the observations required to run the models. The model discussion and associated catalogue in Appendix A are the result of a comprehensive survey conducted by the assessment team. While not every available model was included, the collection is representative of the range of models and allows identification of observations needed to drive the corresponding types of predictive SEP modeling. Section 10.2 further discusses modeling approaches.

The model survey and discussion pertain to current capability and models in development. The assessment team made no attempt to project the path SEP research and modeling may take in the long term. The assessment does not attempt to estimate what new types of observations may be required to support future efforts. As an example, characterizing the multiscale magnetic field throughout the solar corona is important for understanding and modeling solar eruptions. However, remote mid- to upper-coronal magnetic field measurements do not yet exist (e.g., photospheric magnetic field measurements quantify conditions at the bottom of the solar corona) and were not considered in this assessment. This report provides a snapshot of modeling work that was ongoing at the time of the assessment.

10.1 Types of Models

Due to generally increasing interest in space weather, there has been rapid growth in a number of predictive solar eruption, heliospheric plasma, and SEP models. The maturity levels of these models range from current use in operations (e.g., solar wind and transient prediction models used by NOAA) to initial research ideas. Accurate modeling and prediction of SEPs is a major challenge, and the performance of available models leaves room for improvement. However, promising paths for predictive SEP modeling have been identified and are being actively explored by the space weather community. New emphasis on human spaceflight SEP modeling needs is further fueling ongoing development efforts. One of those efforts is the SEP scoreboard curated by the Community Coordinated Modeling Center.[1] The SEP scoreboard is an international effort to compare model performance in a real-time environment and distill new research to address the SEP prediction challenge.

As in Section 9, models are discussed in three categories: pre-eruption, post-eruption, and post-eruption time profile. The report discusses the general approaches to modeling in each category, overall maturity, and observations required to drive the models. The following discussion is accompanied by the model catalogue in Appendix A. The catalogue was developed from a survey of existing modeling capabilities. While not all available models have been captured in the catalogue, the key types of models are represented, and, most importantly, the key observations required for driving different types of models are captured. The model catalogue indicates the priority of modeling types. From an operational utility standpoint, the importance and priority of model types places pre-eruption at priority 1, post-eruption at priority 2, and post-eruption time profile at priority 3. Model maturity was assessed using the ARL framework.

[1] https://ccmc.gsfc.nasa.gov/challenges/sep.php

ARLs are a modification of well-known Technology Readiness Levels: ARL 1 indicates an initial research idea; ARL 9 denotes usage of product in operations. For more details on ARLs in the space weather context, see Pulkkinen et al. [ref. 28].

10.1.1 Pre-eruption Models

Pre-eruption models provide information about pending eruptions. This model category is considered the highest priority, as it provides the largest available lead time and allows mission plan adjustments and short lead-time reactions. Available pre-eruption models have been tuned to predict eruptions 24 hours in advance, while the need is for 6- and 24-hour prediction windows. “Eruption” in this category usually means a solar flare occurred; models for SEP events and coronal mass ejections (CMEs) have also been developed [ref. 29].

Pre-eruption modeling is driven by remote solar observations and photospheric magnetographs that provide information about the state and evolution of solar active regions. While photospheric line-of-sight (LOS) magnetic field measurements are easier to carry out and the most widely used observational input, vector field measurements, such as those conducted by Solar Dynamics Observatory (SDO)/Helioseismic and Magnetic Imager (HMI) instruments, are already used by some of the pre-eruption models. Solar continuum measurements are used in conjunction with photospheric magnetic fields. Since solar flaring history of active regions may contain important information about future eruption, some models also use soft X-ray observations as input (e.g., single-pixel light curves).

Predicting solar eruptions is one of the greatest challenges in space weather research. The best available predictive models provide probabilistic characterization of the likelihood of an eruption, and it is quite possible that due to the complexity of the phenomenon, deterministic predictions are not achievable in practice. Consequently, it appears that probabilistic approaches are a good way forward, and it is encouraging that several available models have reached a fairly high level of maturity. Rigorous validation and prototyping in a real-time environment are necessary to gain confidence in the operational utility of these models.

10.1.2 Post-eruption Models

Post-eruption modeling takes place after an eruption has been observed in the solar corona. The first category of post-eruption models, priority 2 type, pertains to short lead-time predictions that provide estimates for the onset time of the SEP event and the expected peak proton flux. These models use information about the observed flare soft X-ray flux, flare location, and initial signature of the SEP flux level enhancement at the location of interest. Ground-based solar radio observations of Type II and III bursts are also used to guide some of the models.

Depending on the signal used to carry out the prediction, available post-eruption models can potentially provide 30-90 minutes of lead time for SEP onset and peak flux of the event. Many of the existing models have been tuned to predict greater than 10 MeV proton flux. As 10 MeV protons move slower than 100 MeV protons, lead time can be less for the more energetic portions of the SEP spectrum.

While white-light coronagraph observations of coronal mass ejections (CMEs) are not used by most of the more mature post-eruption models, a growing number of efforts integrate CME information into the SEP flux assessments [ref. 30 and references therein]. In addition, lower-corona CME detections that in principle could provide longer SEP prediction lead times than space-based mid- or outer-corona observations can also be carried out from the ground [ref. 31].

Ground-based CME observations can be an attractive complement to the more expensive space-based observations.

10.1.3 Post-eruption Time Profile Models

The second category of post-eruption model, priority 3 type, pertains to predictions of SEP flux as a function of time, including indication of duration of events (see Figure 9.0-1). Empirical models in this category use the same input information as those in the post-eruption category.

The post-eruption time profile modeling category is no exception to the general finding that predicting SEP events and their evolution is a challenging task, and further development and evaluation of model performance is necessary. Perhaps the most promising development effort is the coupling of physics-based magnetohydrodynamic (MHD) heliospheric plasma and shock models with SEP generation and transport models [ref. 32]. This type of coupled physics-based modeling can characterize SEP time profiles throughout the heliosphere. For this next-generation SEP time profile modeling, coronagraph observations are critical for driving the initiation of CMEs and shocks in the MHD models.

10.1.4 Solar Wind and CME Transport Models

Physics-based solar wind and CME transport models perform two roles: 1) Like post-eruption models, they can provide MHD shock information for next-generation SEP time profile modeling, and 2) they can provide general heliospheric space weather situational awareness. Situational awareness in this context means information about the background solar wind conditions and propagation of CMEs throughout the heliosphere. While not included in the list of the three highest priority modeling categories, this kind of situational awareness is important because the background solar wind and transients propagating in it control the generation and transport of energetic particles in the heliosphere.

Observational input to the solar wind and CME transport models include photospheric magnetic field used to build the background wind; coronagraph observations used to insert transients in the models; and possible additional information, such as the extreme ultraviolet (EUV) imagery used to assist the analysis of CME kinematic properties.

10.1.5 Space Environment Effects Models

Space environment effects models are used for spacecraft design and anomaly investigation. Some effects models are described in Appendix A. This assessment assumes an architecture timeline that begins after the spacecraft design phase. While space environment effects models are not used to define the space weather architectures described in this report, these types of models, used in the scientific/engineering community for design and effects mitigation, are included for completeness.

These models focus on space weather effects caused by energetic particles rather than other space environment effects, such as meteoroid impacts. Spacecraft charging can occur on the outer material (i.e., surface charging) or inside the material (i.e., internal charging). Radiation damage is caused by higher energy and heavy ions that penetrate further into the spacecraft. The greater the energy of the particle, the further it can penetrate. As an example, a 100 MeV proton can penetrate approximately 2 inches of aluminum.

Figure 10.1-1 shows an approximate range of particle energies for surface charging, internal charging, and radiation damage. The effects caused by spacecraft charging can include

electrostatic discharge, electromagnetic interference on communications devices, and physical damage of materials. Radiation effects include SEE, TID, and DDD. SEE can cause soft or hard errors in the spacecraft circuitry. TID results in the degradation of microelectronics, and DDD can damage electrical components.

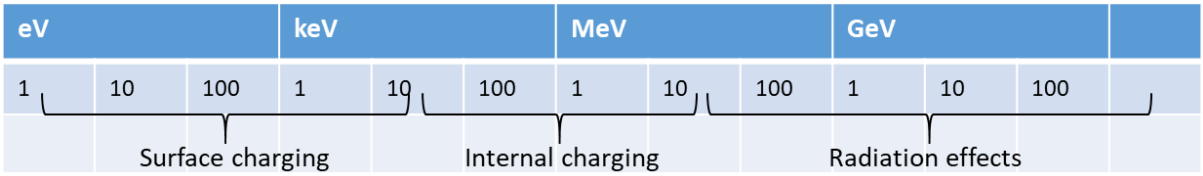

Figure 10.1-1. Approximate Range of Charged Particle Energies for Space Environment Effects

Depending on the type of effects being investigated, input can be plasma density and temperature to flux over a range of energies for electrons, protons, and heavy ions. Additionally, information on spacecraft configuration and material properties is needed to assess how the charged particle environment interacts with the spacecraft components.

10.2 Model Discussion

Predictive space weather modeling, including SEP modeling, is still in the early stages of development. Reflecting the state of understanding of space weather phenomena, most of the currently available predictive SEP models are empirical in nature. There is no first-principles capacity for predicting solar eruptions in the pre-eruption modeling context. However, the field is evolving rapidly and new investments by NASA, the National Science Foundation, and the DoD are allowing new focus on the applied sciences angle of SEP modeling. As an example, the NASA Space Weather Science and Applications (SWxSA) Program is funding SEP-related operations-to-research (O2R) projects that ultimately will enhance predictive capabilities.

Due to ESA and European Union support for applied sciences space weather work over the past 10 years, many of the more mature SEP prediction models are European. In the basic research domain, sharing of information and models across national boundaries is commonplace and part of the scientific process. However, when models become applied and ultimately operational, intellectual property considerations and other related factors can complicate access to and usage of international resources. Consequently, it is imperative that robust U.S.-based modeling capacity be established and maintained through research and analysis (R&A) and research-to-operations-to-research (R2O-O2R) programs, such as SWxSA.

Although space weather and SEP modeling are in the early stages of development, a range of promising modeling approaches and paths forward have been identified by the space weather community (see Appendix A). Identification of the key modeling approaches allows identification of the types of observations that will be required to run the predictive SEP models. The observations identified in this section drive the instrument requirements discussed in Section 11.

11.0 Space Weather Architectures

This section describes space weather architectures for lunar and Mars missions, using findings about operational mitigation procedures, necessary models, and associated observations. It includes a bridging strategy using the ISS and Gateway Programs to best position the Agency for the mission to Mars.

When the action to develop a space weather architecture was assigned, one of the tasks included defining costs "with an emphasis on the most cost-effective solutions that leverage existing national operational space weather infrastructure." This study completed this task by describing different levels of complexity (e.g., baseline, enhanced, and comprehensive). As the architecture assessment proceeded, it became clear that a comprehensive analysis of cost could not be performed. The NESC assessment team determined that the cost of the following architecture options depends on instrumentation priorities and the level of instrument requirements. Further, many of the current assets have or will reach their mission limits. Several instruments continue to operate beyond their planned mission length (e.g., Advanced Composition Explorer (ACE)), but planning a sustained architecture around these platforms would not be wise. These instruments will need replacing at some level. Additionally, some assets may no longer meet program needs and will be phased out. However, the cost of those missions at the given complexity and technology level will serve as a rough estimate for their replacement. Advances in modeling, technology, and forecasting will continue. Costs associated with these advancements may result in higher or lower overall expense for the Agency for any given architecture. In addition, future collaborative activities with other agencies or space programs may lower costs. Once an architecture option is selected, a thorough cost analysis must be conducted, considering the above factors and more.

Throughout this section, the baseline, enhanced, and comprehensive instrument packages for Sun-Earth line (e.g., lunar) and Mars-bound vehicles are referenced. *Baseline* signifies the minimum set of observations and corresponding instruments necessary to support the operational mission timeline in Section 9.0. *Enhanced* (goal) means the desired collection of observations and corresponding instruments providing complete support of the operational mission timeline and overall space weather situational awareness. *Comprehensive* indicates the ideal instrumentation for space weather observations. Baseline, enhanced, and comprehensive instrument complements for the Sun-Earth line package, bridging missions, and Mars missions are summarized in Table 11.1-1.

The Sun-Earth first Libration point (L1) satellite would ideally provide electron and proton energetic particle instruments, coronagraph, vector magnetograph, EUV imager, X-ray sensor, solar wind parameters, magnetic field, decameter-hectometric radio waves, heliospheric imager, and EUV/far ultraviolet (FUV) solar spectral irradiance. In the comprehensive Mars architecture (Section 11.2.3), the architecture suggests three identical satellites at 1 AU 120° apart with goal instrument complement. The team discussed additional locations, notably the other Libration points for Earth. These are summarized in Table 11.1-1, which notes the exploratory science missions that serve as heritage for measurement strategies at these vantage points. The L2 point is considered useful for astrophysics missions, but no apparent use was identified for space environment applications. L3, L4, and L5 were explored by the twin STEREO spacecraft and, although they drifted through these locations, they demonstrated the utility of numerous techniques that have been deployed only at L1 previously. Recently international partners have studied a mission to L5 to enhance space weather forecasting of geomagnetic disturbances.

11.1 Lunar Architecture

As discussed in Sections 9 and 10, the space weather information required to support human and robotic exploration in the cislunar environment and on Mars can be divided into a flow of segments: the forecasts and real-time information required by the operations team to make decisions, the models and tools to derive those forecasts and information, and the observations

needed as inputs into the models and decision aids. The SEP energy/flux thresholds for crewed vehicles needed for the models and decision aids were discussed in Section 4. For robotic exploration, it is assumed spacecraft are designed and built to standards such that SEPs will not affect the vehicles.

Table 11.1-1 captures the space weather architecture for lunar missions. It lists the mission concepts of operations phases and corresponding models, including corresponding model measurement requirements and associated instrument requirements. The table indicates overall mission requirements for the architecture and existing assets. For example, all-clear pre-eruption forecasting models use magnetic field maps and continuum images from NASA's SDO. Operational magnetic field maps are produced by the Global Oscillation Network Group (GONG), jointly run by NOAA and the National Solar Observatory. GONG maps are of lower quality than SDO's research-grade maps, and work is needed to determine how all-clear models will perform with reduced spatial resolution. Operational white light/continuum images are available. The USAF provides classifications of sunspot groups from its Solar Observing Optical Network (SOON), which provides white light solar imagery. Solar soft X-ray fluxes are measured by NOAA's operational GOES satellites. The final column of Table 11.1-1 lists existing assets that are assumed to be available for the Artemis Lunar 2024 target date. However, many of the research assets are nearing or have passed their mission lifetime, or are not considered "operational," meaning real-time data availability is not guaranteed.

Table 11.1-1. Lunar Architecture for Launch, Cruise, Orbit, and Surface Phases

Con-ops Component	Modeling Objectives	Modeling Requirement	Measurement Requirement	Instruments Required	Mission Requirements	Existing Assets, Assumed Available for Lunar 2024
Mission planning and situational awareness (launch, EVAs)	Pre-eruption modeling	24-hour/ 6-hour lead-time forecast of solar eruptions (flare, SEP, CME) Probability of >10 MeV p+ NOT exceeding 10-100 pfu or >100 MeV, not exceeding 1 pfu in next 24 or 6 hours	Photospheric magnetic field LOS or vector)	Photospheric magnetograph	Carry out all measurements along Sun-crewed vehicle line (Sun-Earth line for lunar missions), or close to line 100% instrument and modeling duty cycle for soft X-rays 24/7 observational and modeling data feeds	GONG (operational), SDO/HMI (research)
			Solar continuum/ white-light	Continuum/ white-light solar imager		SOON (operational), SDO/HMI (research)
			Solar soft X-ray	Soft X-ray spectrograph		GOES (operational)
Deploy and enter storm shelter or return to lander	Post-eruption modeling	SEP onset time prediction	Solar soft X-ray	Soft X-ray spectrograph		GOES (operational)
		SEP peak flux prediction	Flare location	EUV imager/ H-alpha imager/ X-ray imager		GOES (operational), SDO/AIA (research)
			Energetic protons	Energetic charged particle detector		GOES (operational)
			CME parameters	Coronagraph		SOHO/LASCO (research), Stereo/COR (research)
		Probability of >10 MeV p+ exceeding 10-100 pfu or >100 MeV p+ exceeding 1 pfu	(Interplanetary) Energetic electrons	Energetic charged particle detector		SOHO/COSTEP (research), ACE/EPAM (research)
			Solar radio bursts (Type II & III)	Solar radio telescope		Ground-based Radio Solar Telescope Network (operational)
			CME parameters	Coronagraph		SOHO/LASCO (research), Stereo/COR (research)

Con-ops Component	Modeling Objectives	Modeling Requirement	Measurement Requirement	Instruments Required	Mission Requirements	Existing Assets, Assumed Available for Lunar 2024
Inform crew about expected evolution and end of SEP event	SEP Time profile/ duration; post-threshold SEP event model/ determine CME arrival	Flux as function or estimate of time below threshold) for >10 MeV p+	Energetic protons	Energetic charged particle detector		GOES (operational), ACE (research)
			CME parameters	Coronagraph		SOHO/LASCO (research), Stereo/COR (research)
Nowcasting	NA	NA	Flux at >10 MeV p+, >30 (or >50) MeV p+, >100 MeV p+	Energetic charged particle detector		GOES (operational), ACE (research)

The assessment team determined that NASA needs no additional assets for space weather/radiation sensing and measurement for operations to, near, or on the Moon. However, this assumes the continued functioning of research missions now in operation, several of which are well beyond their mission operations life (e.g., ACE). If any of these missions or instruments were to fail, the ability to adequately model and/or forecast space weather events would be severely compromised. The precarious future of these instruments has been identified at the national level in the White House Office of Science and Technology Policy by the Space Weather Operations, Research, and Mitigation Committee and in the Space Weather Action Strategy & Plan [ref. 27]. NOAA's Space Weather Follow-On, scheduled for launch in 2024, will provide operational continuity for solar wind and white light coronagraph observations. The following sections describe the baseline, enhanced, and comprehensive instrument packages suggested for Sun-Earth line missions in support of human space exploration. These packages can be flown with the crewed vehicle. An estimated cost was not assigned, but the level of funding required would increase with each package.

Baseline: Photospheric magnetic field maps, energetic ions and electrons, soft X-ray flux with flare location detection.

Enhanced: Baseline package measurements, white-light coronal emissions, and in-situ magnetic field and solar wind plasma.

Comprehensive: Enhanced package plus space-based solar radio (e.g., Type II, Type III) measurements.

Although no new types of instruments are required, continued work in maturing predictive SEP modeling and prediction will be essential. This means work and support for these areas should be continued at the present level.

The team considered the threat posed by solar activity that occurs beyond the west limb of the Sun, not visible from a near-Earth location. Because the magnetic field lines from the Sun are curved as the solar wind expands into the solar system (representing the "Parker Spiral"), these eruptions can produce energetic particles that affect the Earth and Moon with little to no warning. In fact, one of the events (9/29/89) in Table 8.1-2 occurred behind the west limb of the Sun, and overall about 25% of all SEPs arise from behind the limb [ref. 30]. The situation is

somewhat mitigated because forecasters will have tracked solar active regions as they crossed the Sun's visible disk. There remains some risk for active regions that emerge beyond the West limb, but the frequency will be tied to the phase of the solar cycle and the window of exposure is a few days. Active regions that have emerged on the Sun's far side can also produce energetic particles when they appear on the east limb, but the magnetic connections to Earth are poor and research indicates that only about 5% of these are detectable.

A confounding concern for activity occurring beyond the Sun's west limb is the fact that many of the pre-eruption and post-eruption models described here will not have the necessary measurements to drive them. Magnetic field measurements of the solar disk become unreliable because of foreshortening effects near the Sun's limb, and they will not be available for longitudes beyond the west limb. Similarly, soft X-ray light curves that drive many of the models described here will be occulted or not visible at all. Of course, all these concerns would be mitigated with an appropriate L4 monitor.

Two measurement techniques that do appear to work with a near-Earth location are the energetic electrons that precede the more damaging protons, since they will follow the Parker Spiral field lines and arrive before the low to moderate energy protons. Also, coronagraphs will detect CMEs beyond the west limb, and those fast events with no associated activity on the Sun's visible disk can be an indicator of an impending energetic particle storm.

11.2 Mars Architecture

When examining potential concepts of operations for Mars human exploration, the same components of forecasts and real-time information will be required:

1. General mission planning and situational awareness.
2. Decision to deploy and enter a storm shelter or, in the surface phase, return to lander.
3. Information about the evolution and expected duration of SEP event.
4. Nowcasting of the crew radiation dose.

The concept of operations elements, models, and observations for the Mars architecture are the same as described in Table 11.1-1. For the transit to Mars, vehicle concepts and designs are not sufficiently developed to assess detailed shelter concept of operations. Because of the additional time necessary (i.e., 2030s) to develop countermeasure technologies (e.g., shielding, medical) and potential larger mass/volume allowed in a transit vehicle for radiation countermeasures, prediction of space weather impacts to crewed Mars vehicles would be vital to ensure crew safety for these long-duration design reference missions.

Due to the orbit of Mars, instrumentation along the Sun-Earth line will not be sufficient. At times, the crew will be susceptible to SEP events originating from the far side of the Sun. Available instrumentation (e.g., located with the crew or in a Mars orbit) and existing models are capable of providing space weather forecasting at the current state of the art. Given optimal outbound and inbound travel paths, monitoring assets at the Sun-Earth L1, L4 and L5 may provide sufficient additional warning. The Sun-Mars Libration points represent additional locations for environmental architects to consider in the future. A platform at Sun-Mars L1 would provide upstream monitoring for activities on and near the planet, and combined with Sun-Earth Libration monitors, may be sufficient to provide adequate protection. Such an idealized concept is shown in Figure 11-2.1. The time frame for Mars missions is far enough in the future that it is reasonable to expect significant advances in space weather instrumentation

and modeling. As a result, lower-ARL models listed in Appendix A have the potential to support Mars missions.

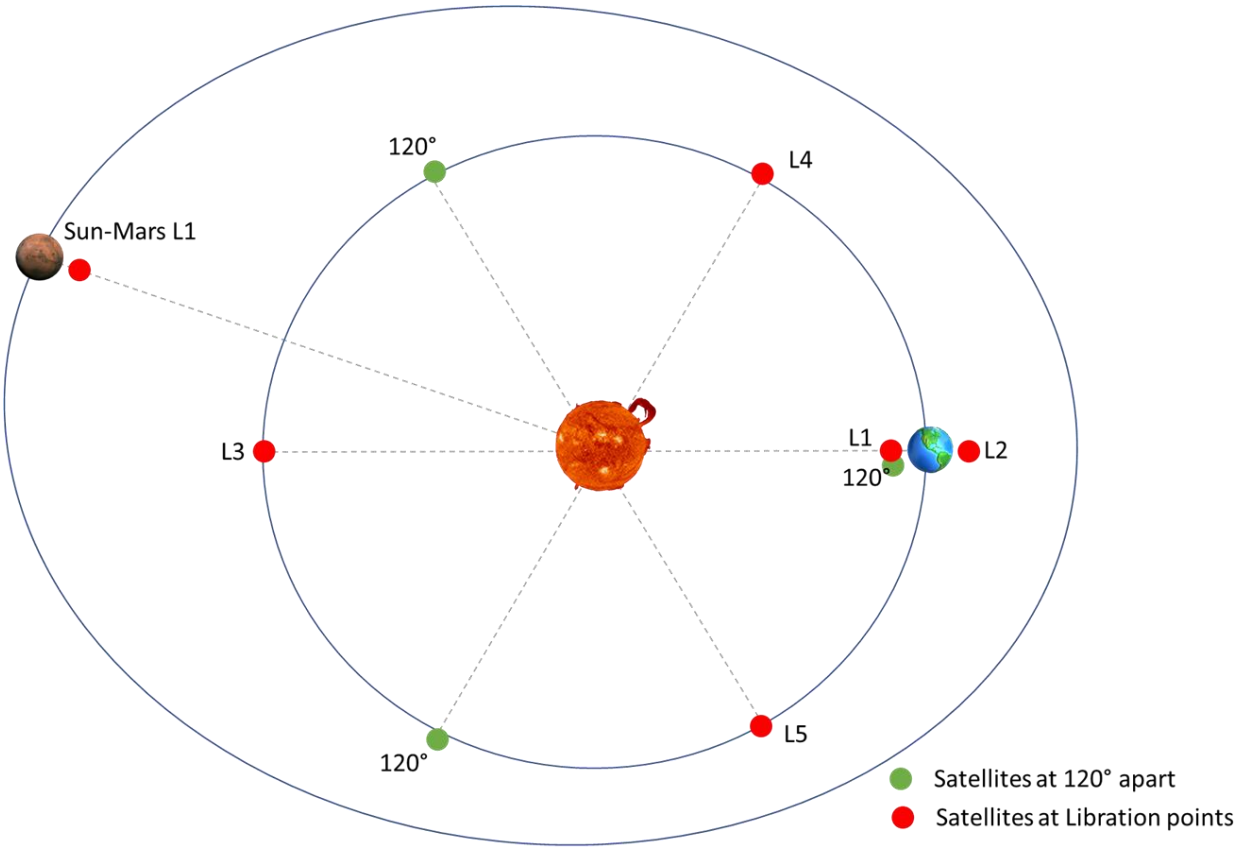

Figure 11.2-1. Concept for Future Monitoring Locations

11.2.1 Mars Baseline Architecture

It is assumed that instrumentation now available to support lunar missions will continue to be available on the Sun-Earth line for Mars missions. The baseline architecture for Mars includes this sustained Sun-Earth line baseline and adds a suite of instruments on the Mars vehicle. This suite includes instrumentation to provide:

- Solar photospheric magnetic field maps
- Solar soft X-ray fluxes and flare location
- Energetic ion and electron spectra and fluxes

11.2.2 Mars Enhanced Architecture

The enhanced architecture for Mars includes the sustained Sun-Earth line enhanced package and an improved suite of instruments on the crewed Mars vehicle. The enhanced instrumentation includes the Mars baseline instrumentation, plus:

- White-light coronal imaging
- In-situ magnetic field
- Solar wind plasma properties
- Space-based radio measurements

11.2.3 Mars Comprehensive Architecture

The comprehensive architecture for Mars includes the sustained Sun-Earth line baseline instruments and separate interplanetary space weather spacecraft. These would be a constellation of three spacecraft at 1 AU and 120° apart in a solar orbit (two additional spacecraft in addition to the Sun-Earth line observations). For example, spacecraft at L3, L4, and L5 would provide such optimal coverage of solar longitudes, which would complement measurements along the Sun-Earth line provided from spacecraft at L1. Each spacecraft would have the same comprehensive set of remote sensing and in-situ instruments supporting advanced space weather modeling and forecasting for Earth and Mars. Possible additional instrumentation on all three spacecraft could include:

- Solar EUV imager
- Heliospheric imager
- EUV/FUV solar spectral irradiance
- Intravehicle dosimeter

11.3 Bridging Strategy to Meet Mars Architecture

11.3.1 ISS Platform

The ISS has operated as a research laboratory for nearly 20 years, and is expected to continue through 2024. In addition to its array of internal research instruments and capabilities, several exterior attachment points can accommodate scientific payloads for a variety of studies. When used in conjunction with solar pointing mechanisms, some of these positions would provide excellent locations for validating advanced instruments (e.g., coronagraph, magnetograph) for use on future crewed vehicles (e.g., Gateway, Mars transit vehicle) and science missions on and off the Sun-Earth line.

11.3.2 Gateway Phase I

To best monitor the top-priority space weather effects, an instrument package detecting energetic charged particles may be deployed on the Gateway Phase I platform. To best categorize and understand the charged particle environment for future lunar and Mars missions, the instruments should be able to measure electrons and ions. Using Phase I as a particle instrument proving ground will provide relevant lessons for a Gateway Phase II instrument package. The Gateway Phase I instrument priority is energetic ions and electrons.

11.3.3 Gateway Phase II

As a part of Gateway Phase II activities, supporting space weather instrumentation should be expanded to cover at least the baseline, but preferably the identified enhanced instrumentation listed in Section 11.2.2. These instruments consist of hosted payloads mounted outside the crewed platform. Importantly, all the technology, processes, and lessons learned gained from implementing this Phase II strategy would be directly transferrable for missions to other planetary targets, such as Mars. Gateway Phase II instrument priorities would be:

- Solar photospheric magnetic field maps
- Solar soft X-ray fluxes and flare location
- Energetic ion and electron spectra and fluxes
- White-light coronal imaging
- In-situ magnetic field

- Solar wind plasma properties
- Space-based radio measurements

11.3.4. Mars Missions

The administration's future human space exploration plans propose going to Mars after the Moon (i.e., Moon-to-Mars). While the NASA plan focuses first on establishing a permanent human presence on the Moon within the next decade, it would be prudent to plan infrastructure to support human exploration to the Moon or Mars, including space weather nowcasting and/or forecasting capabilities. A cost-effective solution that can be pursued now is ride-shares with planned or future Mars missions. An example is the Radiation Assessment Detector (RAD) onboard the Mars Science Laboratory Curiosity Rover, which has provided radiation environment measurements during cruise and at the Martian surface. The successful RAD program demonstrates a cost-effective means by which SMD and HEOMD can collaborate to provide valuable space weather data for future human exploration. The Mars 2020 mission is expected to launch in July/August 2020, and Mars sample return mission(s) are planned for the later 2020s. The assessment team is not aware of a plan to send space weather instruments with these missions. If this continues, valuable opportunities will be lost to obtain space weather data on the transit to or on the surface at Mars. Instrumentation priority would be to fly instrumentation as a hosted payload on a planetary Mars science mission.

11.4 Summary of Architectures

Table 11.4-1 summarizes the architectures resulting from this study for Lunar 2024, Mars missions, and a bridging strategy for Gateway. This report does not discuss costs, which would be deeply dependent upon instrumentation priorities and requirements and on emerging technologies. Many existing assets are aging and will need to be replaced at some instrumentation level. Additionally, some assets may no longer meet program needs (e.g., GONG, SDO, ACE, SOHO).

Table 11.4-1. Summary of Architecture Instrumentation Requirements

HEO Mission Target	Classification	Description
Moon	Lunar 2024	No additional hardware required over the existing NOAA & USAF assets. However, lunar platform should be used as a proving ground for future Mars missions (see Bridging Missions).
Mars	Baseline	Sustained Sun-Earth line assets. Crewed vehicle flying with Mars baseline instrumentation.
	Enhanced	Sustained Sun-Earth line instrumentation. Crewed vehicle flying with Mars enhanced instrumentation.
	Comprehensive	3 spacecraft 120° apart @ 1 AU; all spacecraft have the same remote sensing and in situ instrumentation.
Bridging Missions	ISS Platform	Proving ground for the Lunar/Mars mission. Instrument priorities: magnetograph, coronagraph.
	Gateway Phase I	Energetic charged particle sensors.
	Gateway Phase II	Develop a Mars vehicle instrument package using lessons learned from the ISS proving ground and Phase I.
	Mars	Instrumentation flying as a hosted payload on robotic Mars science missions.

12.0 Findings, Observations, and NESC Recommendations

12.1 Findings

The following findings were identified:

Operations

F-1. The 6-hour all-clear forecasts of >100 MeV protons are useful for launch commitment and routine internal vehicle human mission operations. [Section 9.0]

F-2. The 24- and 6-hour all-clear forecasts of >10 MeV protons are needed for EVAs. [Section 9.0]

F-3. Predictive information in 10–30 minutes lead time would allow shelter deployment to minimize crew exposure. [Section 9.0]

Model development

F-4. A growing number of space weather modeling efforts integrate CME information into the SEP flux assessments, using white-light coronagraph observations of CMEs. [Section 10.1]

Instrumentation

F-5. It is uncertain whether GONG magnetogram quality is sufficient for pre-eruptive all-clear forecasts. [Section 11.4]

F-6. Magnetograms from SDO and GONG may not be available starting in 2024. [Section 11.4]

F-7. Plans for upcoming Mars missions have no space weather instrumentation. [Section 11.3.4]

F-8. Due to the orbit of Mars, instrumentation along the Sun-Earth line will be insufficient. [Section 11.2]

F-9. An instrument package to characterize and understand the energetic charged particle environment, including protons, electrons, and ions, will minimally monitor space weather effects in the near-term. [Section 11.3.2]

F-10. Using protons with energies to 1 GeV would incorporate additional hard spectra variance. [Section 8.2.3]

F-11. Lower corona CME detections that in principle can provide longer SEP prediction lead times than space-based mid- or outer-corona observations can also be carried out from the ground. [Section 10.1]

F-12. Stereoscopic coronagraph observations are required for determining three-dimensional properties of CMEs. [Section 10]

General

F-13. The time frame for Mars missions is far enough in the future that it is reasonable to expect significant advances in space weather instrumentation (e.g., reduction in mass, power, and volume) and modeling. [Section 11.2]

F-14. ISS and Gateway Programs provide opportunities for space weather instrument proving grounds for Mars missions. [Section 11.3]

F-15. The time frame for Mars missions is far enough in the future that it is reasonable to expect significant advances in space weather prediction from additional vantage points beyond L1 (*e.g.*, L3, L4, L5, views of Sun's poles). [Section 11]

12.2 Observations

The following observations were identified:

Operations

O-1. During the Apollo Program, GCR and SEP risks were managed with a detailed ground-based observational approach and mitigated by diligent monitoring of radiation exposure and adherence to NASA standards. [Section 7]

Model development

O-2. Only one pre-eruptive forecast model (i.e., Mag4) with SEP all-clear forecast capability was identified. [Section 10.1]

O-3. Rigorous validation and prototyping in a real-time space weather environment are necessary to gain confidence in model operational utility. [Section 10.1]

O-4. Space weather models that have been developed internationally may be difficult to obtain and evaluate for operational use in the United States. [Section 10.2]

Instrumentation

O-5. Magnetograms are critical for pre-eruptive forecasts. [Section 10.1]

O-6. Using Gateway Phase I as a particle instrument proving ground will provide relevant lessons for a Gateway Phase II instrument package. [Section 11.3.2]

O-7. Observations of particles with energies as low as 10 MeV are valuable for EVA operations. [Sections 8.2.2, 8.2.3]

General

O-8. Many of the space-based space weather research assets are nearing or past their mission lifetimes or are not considered operational. [Section 11.1]

O-9. Models and instruments are needed to ensure advance warning time of SEPs for concepts of operations. [Section 9.0]

O-10. Significant advances in the understanding of the space environment (e.g., SEP, GCR), such as modeling, forecasting, biological requirements and risks, and effects on avionics have occurred since the 1970s. [Section 7]

O-11. NASA Standards and Specification documents exist for natural environments and space weather monitoring. [Section 7]

O-12. Instruments at additional vantage points beyond L1 are needed to ensure advance warning time of SEPs for concepts of operations. [Section 9.0, Section 11.1]

12.3 NESC Recommendations

The following NESC recommendations were identified and are directed to HEOMD and SMD unless otherwise identified:

Operations

R-1. Require concepts of operations to provide 10–30 minutes lead time for warning of predicted critical radiation exposure levels to supply adequate time for the crew to build/take shelter. ***(F-3)***

R-2. Ensure model inputs used for operations have a primary data source with a secondary data input for backup. ***(O-2, O-8)***

R-3. Ensure a minimum of 30 minutes of advance warning time for SEPs. ***(O-9)***

Model development

R-4. Ensure researchers focus on modifying predictive models to target the >100 MeV proton fluxes, in addition to >10 MeV. ***(F-1, F-2)***

R-5. Ensure researchers focus on adapting the pre-eruptive models to add an 6-hour window to the 24-hour window. ***(F-1, F-2)***

R-6. Ensure rigorous validation and prototyping efforts in a real-time environment for proving the operational utility of SEP prediction models. ***(O-3)***

Instrumentation

R-7. Determine if GONG magnetograms are adequate for space weather models. ***(F-5)***

R-8. Plans to replace SDO or GONG should be put in place to support space weather architecture beyond 2024. ***(F-5, F-6)***

R-9. Include space weather monitoring instrumentation on robotic Mars missions. ***(F-8)***

R-10. Position a charged particle sensor outside Gateway Phase I. ***(F-9, O-6)***

R-11. Investigate ground-based lower-corona coronagraph observations in SEP predictions. (***F-4)***

R-12. Ensure future space weather architectures can accurately measure proton fluxes from 10 MeV to 1 GeV. ***(F-2, F-10, O-7)***

General

R-13. In accordance with the National Space Weather Strategy and Action Plan, NASA should ensure sustained R&A and R2O-O2R funding for space weather prediction capability development (including SEP). ***(O-4)***

R-14. Fund development to target miniaturization of instruments needed for Mars vehicles. ***(F-13)***

R-15. Provide guidance, including priorities and rationale, for satellite deployment at L1 and additional vantage points at 1 AU for Mars exploration. ***(O-8)***

R-16. Use the ISS and Gateway Programs as an instrument proving ground for Mars missions. ***(F-14)***

R-17. Ensure appropriate space environment design standards and specifications are levied on commercial vendors. ***(O-11)***

R-18. Support national and international efforts to deploy space weather monitoring satellites with appropriate instrumentation at L1 and additional vantage points, such as L3, L4, and L5. ***(F-12)***

13.0 Alternative Viewpoint(s)

No alternative viewpoints were developed in the course of this assessment.

14.0 Other Deliverables

No unique hardware, software, or data packages, outside those contained in this report, were disseminated to other parties outside this assessment.

15.0 Lessons Learned

No lessons learned were identified as a result of this assessment.

16.0 Recommendations for NASA Standards and Specifications

No standards and specifications recommendations were identified as a result of this assessment.

17.0 Definition of Terms

Dose	Amount of ionizing radiation deposited in a material.
Finding	A relevant factual conclusion and/or issue that is within the assessment scope and that the team has rigorously based on data from independent analyses, tests, inspections, and/or reviews of technical documentation.
Fluence	Flux in a given period of time.
Flux	An item (e.g., mass, particle, energy) passing through a unit area per unit time.
Observation	A noteworthy fact, issue, and/or risk, which may not be directly within the assessment scope, but could generate a separate issue or concern if not addressed. Alternatively, an observation can be a positive acknowledgement of a Center/Program/Project/Organization's operational structure, tools, and/or support provided.
Recommendation	A proposed measurable stakeholder action directly supported by specific Finding(s) and/or Observation(s) that will correct or mitigate an identified issue or risk.

18.0 Acronyms and Nomenclature

μ	Mean
σ	Standard Deviation
AA	Associate Administrator
ACE	Advanced Composition Explorer
AFRL	Air Force Research Laboratory
ALARA	As Low as Reasonably Achievable
Al-Eq	Aluminum Equivalent
ARL	Application Readiness Level
ARS	Acute Radiation Syndrome
AU	Astronomical Unit
BFO	Blood-forming Organs
BR	Bartels Rotations
CAD	Computer-aided Design
CM	Crew Module
CME	Coronal Mass Ejection
CxP	Constellation Program
DDD	Displacement Damage Dose
DoD	Department of Defense
DSNE	Design Specification for Natural Environments
EPAM	Electron, Proton, and Alpha-particle Monitor
ESA	European Space Agency
ESTEC	European Space Research and Technology Centre
EUV	Extreme Ultraviolet
EVA	Extravehicular Activity
FAX	Female Adult voXel
FUV	Far Ultraviolet
GCR	Galactic Cosmic Ray
GEO	Geosynchronous
GeV	Gigaelectron Volt
GOES	Geostationary Operational Environmental Satellite
GONG	Global Oscillation Network Group
Gy-Eq	Gray Equivalent
HEOMD	Human Exploration and Operations Directorate
HMI	Helioseismic and Magnetic Imager
IMP	Interplanetary Monitoring Platform
ISS	International Space Station
JSC	Johnson Space Center

LASCO	Large Angle and Spectrometric Coronagraph Experiment
LEO	Low Earth Orbit
LOS	Line of Sight
MAX	Male Adult voXel
MeV	Megaelectron Volt
MHD	Magnetohydrodynamic
MPCV	Multi-Purpose Crew Vehicle
NESC	NASA Engineering and Space Center
NOAA	National Oceanic and Atmospheric Administration
O2R	Operations-to-Research
R2O-O2R	Research-to-Operations-to-Research
R&A	Research and Analysis
RAD	Radiation Assessment Detector
SDO	Solar Dynamics Observatory
SEE	Single-event Effects
SEP	Solar Energetic Particle
SEPEM	Solar Energetic Particle Environment Modeling
SMD	Science Mission Directorate
SME	Subject Matter Expert
SOHO	Solar and Heliospheric Observatory
SOON	Solar Observing Optical Network
SPAN	Solar Particle Alert Network
SRAG	Space Radiation Analysis Group
SWxSA	Space Weather Science and Applications
TEPC	Tissue Equivalent Proportional Counter
TID	Total Ionizing Dose
U.S.	United States
USAF	U.S. Air Force
VSE	Vision for Space Exploration

19.0 References

1. NASA Office of Inspector General. NASA's Efforts to Manage Health and Human Performance Risks for Space Exploration. October 29, 2015. https://oig.nasa.gov/audits/reports/FY16/IG-16-003.pdf
2. Forbush, S.E. (1946), Three Unusual Cosmic-Ray Increases Possibly due to Charged Particles from the Sun, Phys. Rev., 70, 771-772.
3. Anderson, K.A.; Arnoldy, R.; Hoffman, R.; Peterson, L; and Winckler, J.R. (1959), Observations of Low-energy Solar Cosmic Rays from the Flare of 22 August 1958, Journ. Geophys. Res., 64, 1133-1147.

4. Arnoldy, R.L.; Hoffman, R.A.; and Winckler, J.R. (1960), Solar Cosmic Rays and Soft Radiation Observed at 5,000,000 Kilometers from Earth, Journ. Geophys. Res., 65, 3004-3007.
5. Pickering, J.E., and Talbot, J.M. (1963), A Reappraisal of the Radiation Hazards to Manned Space Flight, in Proceedings of the 2nd Manned Space Flight Meeting, April 22-24, 1963, Dallas, TX, published by the American Institute of Aeronautics and Astronautics, New York.
6. Prew, H.E. (1956), Space Exploration—The New Challenge to the Electronics Industry, in Proceedings of the American Astronautical Society, 3rd annual meeting, December 6-7, 1956, New York.
7. Townsend et al., Solar Particle Event Storm Shelter Requirements for Missions Beyond Low Earth Orbit, Life Sciences in Space Research 17, 2018.
8. Hu, S.; Kim, M.-H.Y.; McClellan, G.E.; and Cucinotta, F.A. (2009), Modeling the Acute Health Effects of Astronauts from Exposure to Large Solar Particle Events, Health Physics, 96(4), 1-12.
9. Portree, D.S.F. (2001), Humans to Mars: Fifty years of Mission Planning 1950-2000, Monographs in Aerospace History #21, NASA SP-2001-4521.
10. Anderson, K.A., and Fichtel, C.E. (1961), Discussions of Solar Proton Events and Manned Space Flight, NASA Technical Note D-671, March 1961.
11. Anderson, K.A. (1961), Preliminary Study of Prediction Aspects of Solar Cosmic Ray Events, NASA Technical Note D-700, April 1961.
12. English, R.A.; Benson, R.E.; Bailey, J.V.; and Barnes, C.M. (1973), Apollo Experience Report—Protection against Radiation, NASA Technical Note D-7080.
13. National Research Council (2006), Space Radiation Hazards and the Vision for Space Exploration: Report of a Workshop.
14. National Council on Radiation Protection and Measurements (2006), NCRP Report Number 153, Information Needed to Make Radiation Protection Recommendations for Space Missions Beyond Low-Earth Orbit.
15. National Research Council, (2008), Managing Space Radiation Risk in the New Era of Space Exploration.
16. Jun, I.; Swimm, R.T.; Ruzmaikin, A.; Feynman, J.; Tylka, A.J.; and Dietrich, W.F. (2006), "Statistics of Solar Energetic Particle Events: Fluences, Durations, and Time Intervals," Advances in Space Research, Vol 40., No. 3.
17. Jiggens, P.; Varotsou, A.; Truscott, P.; Heynderickx, D; Lei, F.; Evans, H; and Daly, E. (2018), "The Solar Accumulated and Peak Proton and Heavy Ion Radiation Environment (SAPPHIRE) Model," IEEE Transactions on Nuclear Science, Vol 65, No 2.
18. Slaba, T.C.; Blattnig, S.R.; Badavi, F.F.; Faster and More Accurate Transport Procedures for HZETRN. Journal of Computational Physics, Volume 229, pp. 9397-9417 (2010).
19. Mertens, C.J., and Slaba, T.C. (2019), Characterization of Solar Energetic Particle Radiation Dose to Astronaut Crew on Deep-Space Exploration Missions, Space Weather, accepted with minor revisions.
20. Crosby, N.; Heynderickx, D.; Jiggens, P.; Aran, A.; Sanahuja, B.; Truscott, P.; Lei, F.; Jacobs, C.; Poedts, S.; Gabriel, S.; Sandberg, I.; Glover, A.; and Hilgers, A. (2015), SEPEM: A Tool for Statistical Modeling the Solar Energetic Particle Environment, Space Weather, 13, 406-426, doi:10.1002/2013SW001008.

21. Raukunen, O.; Vainio, R.; Tylka, A.J.; Dietrich, W.F.; Jiggens, P.; Heynderickx, D.; Dierckxsens, M.; Crosby, N.; Granse, U.; and Siipola, R. (2018), Two Solar Proton Fluence Models based on Ground Level Enhancement Observations, J. Space Weather Space Clim., 8, A04, https://doi.org/10.1051/swsc/2017031.
22. Belov, A.; Eroshenko, E.; Mavromichalaki, H.; Plainaki, C.; and Yanke, V. (2005), A Study of the Ground Level Enhancement of 23 February 1956, Advances in Space Research, 35, 697-701.
23. Cramp, J. L.; Duldig, M.L.; Fluckiger, E.O.; Humble, J.E.; Shea, M.A.; and Smart, D.F. (1997), The October 22, 1989, Solar Cosmic Ray Enhancement: An analysis of the anisotropy and spectral characteristics, Journal of Geophysical Research, 102(A11), 24,237-24,248.
24. Plainaki, C.; Belov, A.; Eroshenko, E.; Macromichalaki, H.; and Vanke, V. (2007), Modeling Ground Level Enhancements: Event of January 2005, Journal of Geophysical Research, 117, A04102.
25. Mertens, C. J., & Slaba, T. C. (2019). Characterization of solar energetic particle radiation dose to astronaut crew on deep-space exploration mission. Space Weather, 14, 1650-1658, https://doi.org/10.1029/2019SW002363.
26. Mertens, C. J.; Slaba, T.C.; and Hu, S. (2018), Active Dosimeter-based Estimate of Astronaut Acute Radiation Risk for Real-time Solar Energetic Particle Events, Space Weather, 16, https://doi.org/10.1029/2018SW001971.
27. National Science and Technology Council, National Space Weather Strategy and Action Plan, March 2019.
28. Pulkkinen et al., Geomagnetically Induced Currents: Science, engineering and applications readiness, Space Weather, 15, doi:10.1002/2016SW001501, 2019.
29. Falconer, D.; Barghouty, A.F.; Khazanov, I.; and Moore, R. (2011), A Tool for Empirical Forecasting of Major Flares, Coronal Mass Ejections, and Solar Particle Events from a Proxy of Active Region Free Magnetic Energy, Space Weather, 9, S04003, doi:10.1029/2009SW000537.
30. Richardson, I. G.; Mays, M. L.; and Thompson, B. J. (2018). Prediction of Solar Energetic Particle Event Peak Proton Intensity using a Simple Algorithm Based on CME Speed and Direction and Observations of Associated Solar Phenomena. Space Weather, 16, 1862–1881.
31. Thompson, W.T.; St. Cyr, O.C.; Burkepile, J.T.; and Posner, A. (2017). Automatic Near-Real-time Detection of CMEs in Mauna Loa K-Cor coronagraph images, Space Weather,15, 1288–1299.
32. Luhmann, J.G., et al. (2017), Modeling Solar Energetic Particle Events using ENLIL Heliosphere Simulations, Space Weather, 15, 934–954, doi:10.1002/2017SW001617.
33. NASA (2019), JSC-12820: ISS Generic Operational Flight Rules, Vol. B, Final, PCN-74.
34. GP-10017, Gateway Human-System Requirements (HSR): L2-HSR-6085 was divided into L2-HSR-6085 Ionizing Radiation Protection System, and L2-HSR-6090 Ionizing Radiation Protection System Setup Time.

Appendices

Appendix A. Model Catalogue

Appendix A. Model Catalogue

To review the catalog, please visit the NESC website at https://www.nasa.gov/nesc to request a link to the file.

REPORT DOCUMENTATION PAGE

Form Approved
OMB No. 0704-0188

1. REPORT DATE *(DD-MM-YYYY)*	2. REPORT TYPE	3. DATES COVERED *(From - To)*
04/14/2020	Technical Memorandum	

4. TITLE AND SUBTITLE
Space Weather Architecture Options to Support Human and Robotic Deep Space Exploration

5a. CONTRACT NUMBER

5b. GRANT NUMBER

5c. PROGRAM ELEMENT NUMBER

6. AUTHOR(S)
Minow, Joseph I./ Mertens, Christopher J.; Neergaard-Parker, Linda; Allen John R.; Fry, Dan J.; Semones, Edward J.; Hock, Rachel A.; Jun, Insoo; Onsager, Terrence G.; Kulkkinen, Antti A.; St. Cry, Chris

5d. PROJECT NUMBER

5e. TASK NUMBER

5f. WORK UNIT NUMBER
869021.05.07.12.11

7. PERFORMING ORGANIZATION NAME(S) AND ADDRESS(ES)
NASA Langley Research Center
Hampton, VA 23681-2199

8. PERFORMING ORGANIZATION REPORT NUMBER
NESC-RP-17-01215

9. SPONSORING/MONITORING AGENCY NAME(S) AND ADDRESS(ES)
National Aeronautics and Space Administration
Washington, DC 20546-0001

10. SPONSOR/MONITOR'S ACRONYM(S)
NASA

11. SPONSOR/MONITOR'S REPORT NUMBER(S)
NASA/TM-20205000837Corrected Copy

12. DISTRIBUTION/AVAILABILITY STATEMENT
Unclassified - Unlimited
Subject Category Space Transportation and Safety
Availability: NASA STI Program (757) 864-9658

13. SUPPLEMENTARY NOTES

14. ABSTRACT
NASA's Associate Administrator (AA) for the Human Exploration and Operations Directorate (HEOMD) requested the NASA Engineering and Safety Center (NESC) to conduct an independent technical assessment of space environment monitoring and forecasting architecture options to support human and robotic deep space exploration. This document contains the outcome of the NESC assessment.

15. SUBJECT TERMS
Solar Energetic Particle; NASA Engineering and Safety Center; Deep Space Exploration; Galactic Cosmic Ray; Extravehicular Activity

16. SECURITY CLASSIFICATION OF:			17. LIMITATION OF ABSTRACT	18. NUMBER OF PAGES	19a. NAME OF RESPONSIBLE PERSON
a. REPORT	b. ABSTRACT	c. THIS PAGE			STI Help Desk (email: help@sti.nasa.gov)
U	U	U	UU	60	19b. TELEPHONE NUMBER *(Include area code)* (443) 757-5802